# Adaptive Methods for Efficiency Improvement in Magnetic Resonance based Wireless Power Transmission System

Hoang Minh Huy

Electrical Engineering Program

Graduate school of UNIST

2012

# Adaptive Methods for Efficiency Improvement in Magnetic Resonance based Wireless Power Transmission System

Hoang Minh Huy

Electrical Engineering Program

Graduate school of UNIST

# Adaptive Methods for Efficiency Improvement in Magnetic Resonance based Wireless Power Transmission System

A thesis
submitted to
the Graduate School of UNIST
in partial fulfillment of the
requirements for the degree of
Master of Science

Hoang Minh Huy

05.21. 2012
Approved by

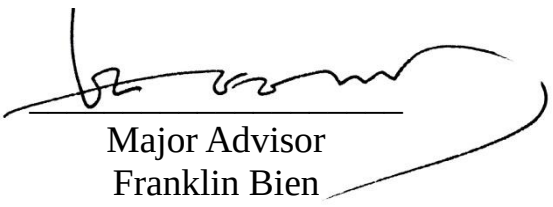

Major Advisor
Franklin Bien

# Adaptive Methods for Efficiency Improvement in Magnetic Resonance based Wireless Power Transmission System

Hoang Minh Huy

This certifies that the thesis of Hoang Minh Huy is approved.

05.21. 2012

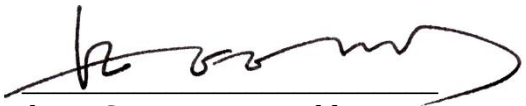

Thesis Supervisor: Franklin Bien

Jingook Kim: Thesis Committee Member #1

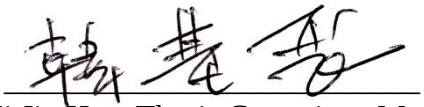

Ki Jin Han: Thesis Committee Member #2

# Abstract

Wireless Power Transmission (WPT) is a cutting-edge technology that signifies a new era for electricity without the need of wires. Wireless power or wi-power is increasingly becoming the main interest of many R&D firms to eliminate the “last cable” after the wide public exposure of Wi-Fi lately. Even though the first idea was devised from Nikola Tesla in the early 20$^{th}$ century, there was never strong demand for it due to the lack of portable electronic devices. In recent years, with the advent of a booming development in cell-phones and mobile devices, the interest of wireless energy has been re-emerged. WPT offers the possibility to supplying power for electronic devices without having to plug them into AC socket. In this thesis, all the perspectives about wireless power transfer from basic fundamentals to in-depth analysis are presented. In addition, adaptive methods for efficiency improvement in magnetic resonant WPT system are proposed to lay down the ground work of innovative power technology and open opportunities to commercially implement the advance WPT system in future.

# Contents

# List of Figures

(a) S21 without axial-misalignment and matching.

(b) S11 without axial-misalignment and matching.

(c) S21 with axial-misalignment and without matching.

(d) S11 with axial-misalignment and without matching.

(f) S21 with axial-misalignment and matching.

**Figure 4-1** Adaptive circuit of frequency control.

**Figure 4-2** Adaptive circuit of impedance matching control in transmitter side.

# List of Tables

# Nomenclature

**AC** Alternating Current.

**ADS** Advanced Design System.

**ALL** Antenna Locked Loop

**EM** Electromagnetic.

**FCC** Federal Communications Commission.

**HFSS** High Frequency Structure Simulator.

**IPT** Inductive Power Transfer.

**ISM** Industrial, Scientific and Medical

**KVL** Kirchhoff's Voltage Law

**MIT** Massachusetts Institute of Technology.

**NASA** National Aeronautics and Space Administration.

**PA** Power Amplifier.

**R&D** Research & Development

**SBSP** Space based Solar Power.

**SSPS** Satellite Solar Power System

**VNA** Vector Network Analyzer.

**WPT** Wireless Power Transmission/Transfer.

# Chapter I

# Introduction

This chapter provides fundamental stuffs of Wireless Power Transmission including definition, how it works, its history and classification and some important figures of merit. Finally, the contribution points of thesis are stated.

## 1.1. Fundamentals of Wireless Power Transmission (WPT)

### 1.1.1. Motivation and Related Work

The motivation for wireless power comes from wires being cumbersome and messy. With the large number of mobile electronics that we own today, there is a demand for convenience in managing their power supplies. Wireless communication has revolutionized the way we interact with communication devices. In a world without wireless communication, we would have to go through the cumbersome process of locating an Ethernet port and then connecting our device to it via a cable before gaining access to the Internet. We are well aware of the convenience that wireless communication brings to us and wireless power will add to that convenience tremendously.

Wireless power transmission (WPT) is a cutting-edge technology that signifies a new era for electricity without a need of wires. Wireless power or wi-power is increasingly becoming the main interest of many R&D firms to eliminate the “last cable” after the wide public exposure of Wi-Fi lately. The concept of wireless power transfer can be traced back to 1820 when Andre-Marie Ampere developed his law which states that an electric current produces a magnetic field. Following the work by Michael Faraday (1830), James C. Maxwell (1864) and Heinrich R. Hertz (1888), Nikola Tesla experimentally demonstrated wireless power transfer in 1891 [1]. His biggest project involved the Wardenclyffe Tower. Although the transmitting tower could be used for wireless communications, it was constructed with the intention to transmit wireless power [2]. In Tesla’s power transmission system, he hypothesized the Earth to be a giant charged sphere that could be driven at its resonant frequency and that he could close the circuit using giant electric fields in the Earth’s ionosphere [1]. Much of his research on wireless power involved radiative electromagnetic waves that are practical for transferring information but pose immense difficulties for wireless power transfer for two reasons [3]. Firstly, omnidirectional radiation is very power inefficient. Secondly, if we were to use unidirectional radiation instead, we would require a direct line of sight and complicated tracking mechanisms.

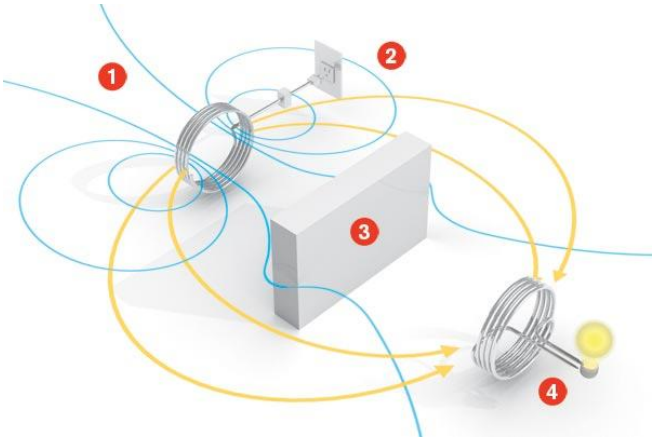


Figure 1-1: Illustration of Wireless Power Transfer.

Although wireless power could have been developed a lot earlier, there was never strong demand for it because of lack of mobile electronic devices then. Commonplace mobile electronics today such as laptops and cellphones have caused a renewed interest in wireless power.

### 1.1.2. Basic Principle

In Tesla's experiment, he designed a resonant circuit that is able to couple a high frequency current into another resonant circuit of a similar structure. With his circuit, he was able to power wirelessly (without any physical interconnecting conductor) a light bulb. The theory behind wireless power transfer is already detailed in the Maxwell's equations:

$$\nabla \cdot D = \rho \tag{1.1}$$

$$\nabla \cdot B = 0 \tag{1.2}$$

$$\nabla \times E = -\frac{\partial B}{\partial t} \tag{1.3}$$

$$\nabla \times H = J + \frac{\partial D}{\partial t} \tag{1.4}$$

The last two curl equations state that a time-varying magnetic flux generates an electric field, and a time-varying electric flux generates a magnetic field. Therefore, if a time-varying electric current can be generates, the time-varying current will induces a time-varying magnetic field. This time-changing magnetic field can "somehow" be picked up and induce a time-varying electric field, or an AC voltage across a receiving load. Tesla's contribution lies on the design of a circuit that can generate/receive a time-varying magnetic field in free-space. It shall be emphasized that Tesla's method is not based on the direct transfer of energy through the use of propagating electromagnetic wave. Tesla's method is actually a near-field method, whereas the use of propagating electromagnetic wave (like transmission

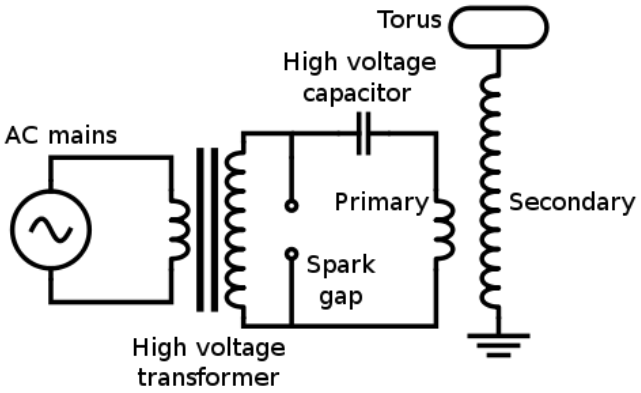


Figure 1-2: Typical Tesla coil schematic.

of microwave power through an antenna) is a far-field method. The two methods differ by the transmission range as well as the angular coverage of the system.

## 1.2. Classification of WPT

According to power transmission distance, wireless transmission can be divided into three categories: short distance, medium distance, and long distance.

### 1.2.1. Short Distance WPT Mode

Short distance mode of WPT indicates that the furthest distance of power transmission is within several millimeters, and the typical representation of such transmission mode is based upon inductive coupling technique, which is also known as inductive power transmission (IPT). The inductive coupling works [4]-[7] under the resonant coupling effect between coils of two LC circuits. The maximum efficiency is only achieved when transmitter and receiver are placed very close from each other.

Figure 1-3: Inductive Power Transfer system.

### 1.2.2. Medium Distance WPT Mode

The furthest distance of medium distance mode is bound to several meters, which mainly includes two categories: ultrasonic and magnetic resonance coupling technique.

- Ultrasonic mode: Ultrasonic is sound wave which frequency is more than twenty thousand Hz and belongs to mechanical wave. Recently, as the enlargement of ultrasonic application in related economy industry, the research about mechanism and application of power ultrasonic technology has achieved comparatively development. Ultrasonic has been practically applied to many fields such as ultrasonic machining and processing technology, ultrasonic detecting and controlling technology. Ultrasonic power transmission utilizes piezoelectric effect and converse piezoelectric effect of piezoelectric material, which can convert mechanical power electrical power, or electrical power to mechanical power, therefore realize the transformation of power, and realize the conversion of ultrasonic power to mechanical power through the vibration of piezoelectric material, consequently realize power transmission. The research about ultrasonic WPT is mainly focused on small power wireless charging system [8], [9].

- Magnetic resonance coupling mode: Through a lot of year's research, research group from MIT invented a kind of completely novel wireless power transmission mode based on magnetic resonance coupling [3],[10]. Resonance induction adopts electromagnetism field Syntony technology, as intrinsic frequencies of receiving antenna is in accord with electromagnetism field frequencies of sending antenna, the resonance will occur and coupling intension of magnetic field will increase. They successfully illumed 60W lamp by locating receiving winding (antenna) to 2m from sending antenna, and transmission efficiency can reach 40% (while distance is 1m, efficiency can reach 90%).

Figure 1-4: Ultrasonic WPT system in [8].

Figure 1-5: Magnetic resonance based WPT system in [3].

### 1.2.3. Long Distance WPT Mode

Transmission of long distance wireless power transmission can reach several decades kilometers, which mainly includes two categories: microwave transmission and laser transmission.

- Laser transmission: The laser beam is coherent light beam capable to transport very high energies, this makes it in an efficient mechanism to send energy point to point in a line of sight. The realization theory of common laser power transmission is simple and very similar to common laser generator and power source. Power source is to provide necessary power to laser generator, the latter convert power into laser power and send it out. Laser receiving equipment is to receive laser from laser generator and convert it into electrical power, which is converse process. When laser irradiate photoelectric converter, the latter can realize the conversion of electrical power from light power. Research spotlight to laser wireless power transmission focus on wireless charging system, Space based Solar Power (SBSP) and Satellite Solar Power System (SSPS) system. NASA introduced in 2003 a remote-controlled aircraft wirelessly energized by a laser beam and a photovoltaic cell infra-red sensitive acting as the energy collector. In fact, NASA is proposing such scheme to power satellites and wireless energy transfer where none other mechanism is viable [11].

- Microwave transmission: Microwave is one kind of electromagnetic wave, whose wavelength is from 1 mm to 1 m, frequency from 0.3 GHz to 300 GHz. The investigation spotlight of microwave WPT mainly focuses on wireless charging, SBSP and SSPS systems [12]-[14]. SBSP and SSPS take advantage of solar power to supply power to earth, planet, and spacecraft, thereby ultimately solve energy source crisis facing to human being. Powercast Co. Ltd has developed production for commercial application by microwave WPT.

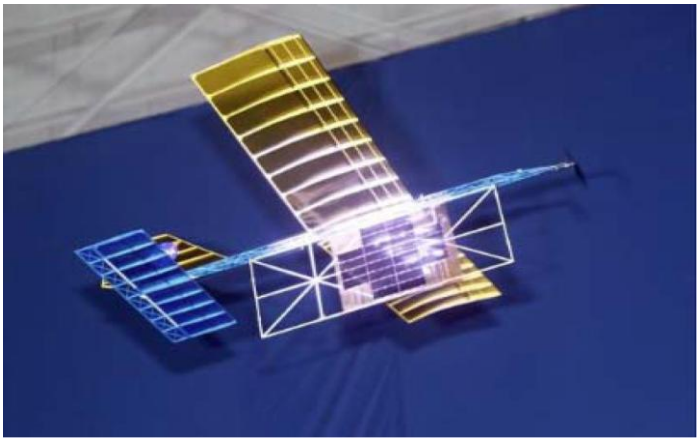

Figure 1-6: Plane driven by laser in [11].


Figure 1-7: MILAX: microwave power was fed to the airplane with lightweight rectennas by a computer-controlled phase-array antenna installed on the roof of a transmitter car [15].

| Transfer method | Distance | Frequency range | Problems | Application |
|---|---|---|---|---|
| **Inductive coupling** | Short distance (~ few millimeters to centimeters) | 125 kHz, 13.56 MHz | Short distance | Tooth brush, etc. |
| **Magnetic resonance coupling** | Medium distance (~ few meters) | ~ 10 MHz | Resonance matching, Coil offsets | TV, Laptop, etc. |
| **Electromagnetic wave** | Long distance (~ kilometers) | Several GHz | Effect on human, directivity | |

Table 1-1: Categories in WPT.

As wavelength of microwave is comparatively long, this made microwave producing serious scattering in long distance transmission, and therefore cause debasement of transmission efficiency. To improve transmission efficiency, microwave power transmission system need bigger sending and receiving antenna, this limits its application range.

## 1.3. Critical Parameters for WPT System Design

### 1.3.1. Transfer Efficiency

Fig. 1-9 shows the calculated optimal achievable efficiency of a system according Fig. 1-8 with the assumption of a quality factor of 100. All dimensions are scaled to the diameter of the larger coil D, which ever it is (transmitter or receiver coil). The values are shown as a function of the axial distance of the coils (z/D). The parameter is the diameter of the smaller coil $D_2$. The figure shows that

- Efficiency drops dramatically at larger distance (z/D > 1) or at a large size difference of the coil ($D_2$/D < 0.3)
- A high efficiency (>90%) can be achieved at close distance (z/D < 0.1) and for coils of similar size ($D_2$/D = 0.5..1)

This shows that inductive power transmission over a large distance, e.g. into a space, is very inefficient. Today, we cannot afford to waste energy for general power applications by using such a system.

On the other hand, the figure shows that inductive power transmission in the proximity of the devices, e.g. at a surface, can be really efficient and competitive to wired solutions. Wireless proximity power transmission combines comfort and ease of use with today's requirements for energy saving.

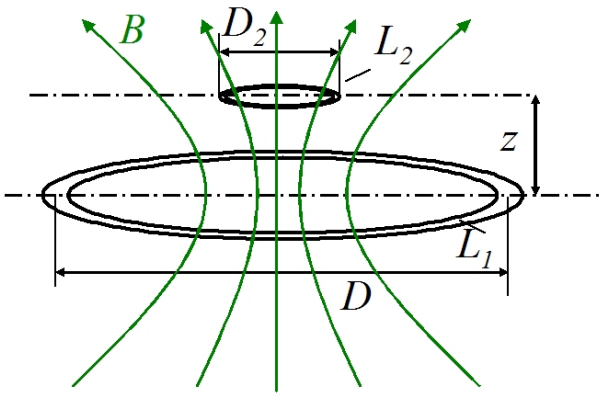


Figure 1-8: Typical arrangement of an inductively coupled power transfer system [16].

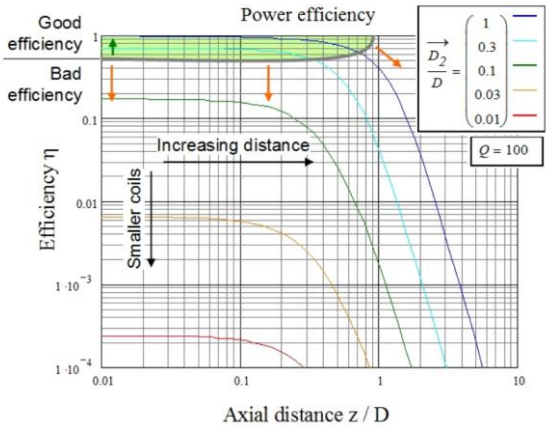


Figure 1-9: Power efficiency for an inductive power transfer system consisting of loop inductors in dependence on their axial distance z with size ratio as parameter, Calculated Q = 100 [16].

## 1.3.2. Quality Factor

The ratio of the inductance L to the resistance R of a coil remains constant for different winding arrangements in the same volume and shape. It makes sense to define this value as a figure of merit to distinguish different coil structures. The quality factor Q is defined by this ratio, which refers to the "goodness" of a reactive component:

$$Q = \frac{\omega L}{R} \tag{1.5}$$

The quality factor Q can have a value between 0 and infinity. But technically it is difficult to obtain values far above 1000 for coils. For mass production you may expect values around 100. A quality factor below 10 is not very useful. These values have to be considered as the typical order of magnitude. The higher Q factor, the narrower the bandwidth and the more selective the circuit is.

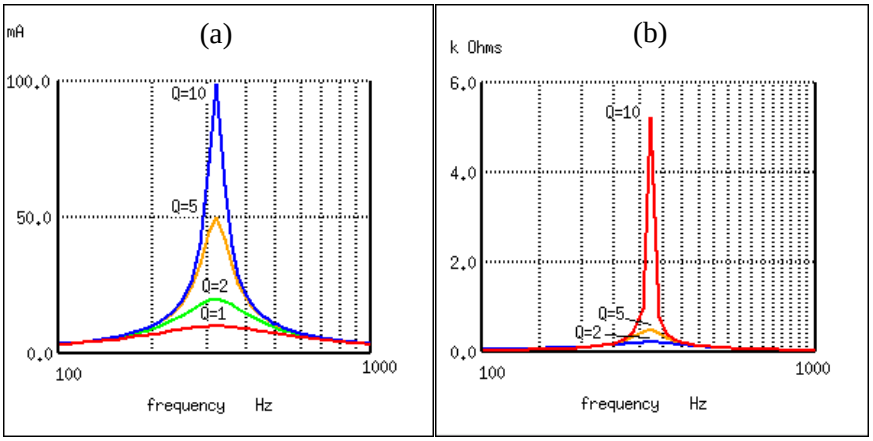


Figure 1-10: Quality factor Q characteristic, (a) series resonance (b) parallel resonance.

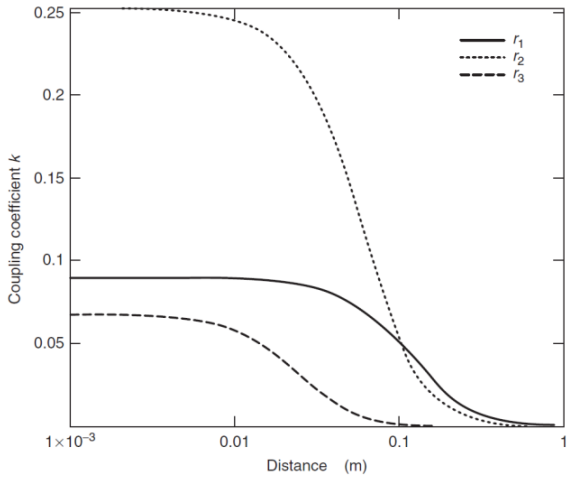


Figure 1-11: Graph of the coupling coefficient for different sized conductor loops. Transponder antenna: $r_{Transp}$ = 2 cm, reader antenna: $r_1$ = 10 cm, $r_2$ = 7.5 cm, $r_3$ = 1 cm [17].

## 1.3.3. Coupling Coefficient

Mutual inductance is a quantitative description of the flux coupling of two conductor loops. The *coupling coefficient k* is introduced so that we can make a qualitative prediction about the coupling of the conductor loops independent of their geometric dimensions. The following applies:

$$k = \frac{M}{\sqrt{L_1 L_2}} \tag{1.6}$$

The coupling coefficient always varies between the two extreme cases $0 \leq k \leq 1$.

- $k = 0$: Full decoupling due to great distance or magnetic shielding.
- $k = 1$: Total coupling. Both coils are subject to the same magnetic flux. The transformer is a technical application of total coupling, whereby two or more coils are wound onto a highly permeable iron core.

For example, in practice, inductively coupled transponder systems operate with coupling coefficients that may be as low as 0.01 (<1%) (Fig. 1-11).

## 1.3.4. Lumped Parameters

### 1.3.4.1. Inductance

The inductance of circular/helical structure can be computed as follows [10]:

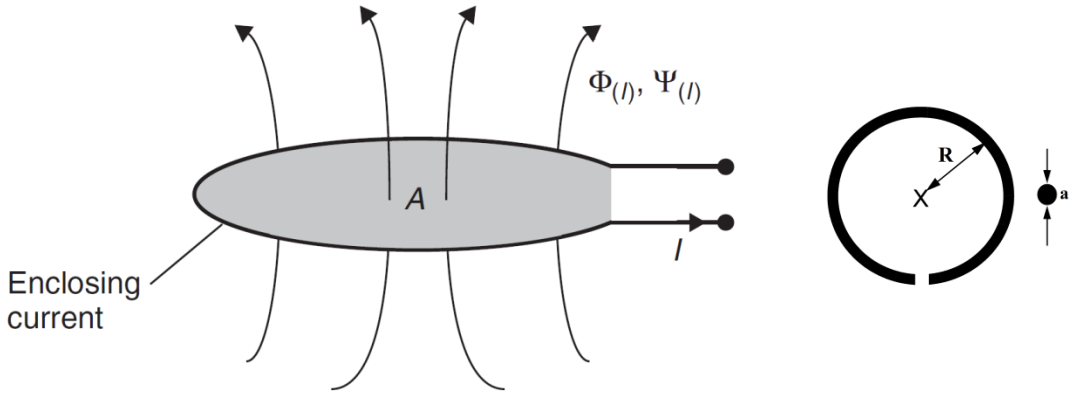


Figure 1-12: Inductance definition.

$$L = N^2 \mu R \left[ ln\left(\frac{8R}{a}\right) - 2 \right] \tag{1.5}$$

Where:

- N : number of turns
- $\mu$ : relative permeability
- R : radius of the coil
- a : radius of the cross section of the coil

Inductance is one of the characteristic variables of conductor coils. The inductance of a conductor coil depends totally upon the material properties (permeability) of the space that the flux flows through and the geometry of the layout.

### 1.3.4.2. Resistance

For a coil with N turns and made of a material with conductivity $\sigma$, the modified standard formulas for ohmic ($R_o$) and radiation ($R_r$) resistances are given as below [10]:

$$R_o = \sqrt{\frac{\mu_0 \omega}{2\sigma}} \frac{l}{4\pi a} \tag{1.6}$$

$$R_r = \sqrt{\frac{\mu_0}{\varepsilon_0}} \left[ \frac{\pi}{12} N^2 \left(\frac{\omega R}{c}\right)^4 + \frac{2}{3\pi^3} \left(\frac{\omega h}{c}\right)^2 \right] \tag{1.7}$$

Where:

- $\omega$ : angular frequency
- c : speed of light

The ohmic losses caused by the AC resistance from currents travelling on the outside of conductor. The skin depth is defined as $\delta = \sqrt{\frac{2}{\omega\sigma\mu}}$, with $\sigma$=5.96 x $10^7$ for copper. For f >10 MHz, the skin depth is $\approx 20\,\mu m$.

### 1.3.4.3. Mutual Inductance

Closed form equations for the mutual inductance of two filamentary (electrically small, with wire radius ≪ coil radius) coils for all physical arrangements have been derived [18]-[20]. Fig. 3.3 shows all relevant variables for calculations.

The relevant equations defining the mutual inductance between two such coils are as follows:

$$M_{12} = \frac{2\mu_0}{\pi}\sqrt{r_1 r_2}\int_0^{\pi} \frac{\left[\cos\theta - \frac{c}{r_2}\cos\phi\right]\psi(k)}{k\sqrt{V^3}}d\phi \tag{1.8}$$

Where:

$$\alpha = \frac{r_2}{r_1},\ \beta = \frac{d}{r_1}$$

$$V = \sqrt{1 - \cos^2\phi\sin^2\theta - 2\frac{c}{r_2}\cos\phi\cos\theta + \frac{c^2}{r_2^2}}$$

$$k^2 = \frac{4\alpha V}{(1+\alpha V)^2 + \xi^2},\ \xi = \beta - \alpha\cos\phi\sin\theta$$

$$\psi(k) = \left(1 - \frac{k^2}{2}\right)K(k) - E(k)$$

Where $K(k)$ and $E(k)$ are complete elliptic integrals of the first and second kind, respectively, as follows:

$$K(k) = \int_0^{\frac{\pi}{2}} \frac{d\beta}{\sqrt{1 - k^2\sin^2\beta}} \tag{1.9}$$

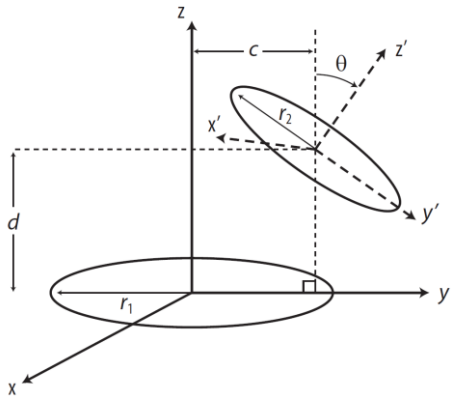


Figure 1-13: Two coils with variable defined for all positions.

$$E(k)=\int_0^{\frac{\pi}{2}}\sqrt{1-k^2\,sin^2\,\beta}\,d\beta \tag{1.10}$$

These equations define the mutual inductance between two coils for any configurations.

**Simplified Mutual Inductance for Co-Axial Coils**

The mutual inductance for two coils aligned co-axially (along the same central axis) as shown in Fig. 1-14 reduces to a less complex equation. The mutual inductance was solved by application of Neumann's relations in [21]. Equation (1.8) reduces to:

$$M_{12}=\mu\sqrt{r_1 r_2}\left[\left(\frac{2}{k}-k\right)K-\frac{2}{k}E\right] \tag{1.11}$$

Where:

$$k^2=\frac{4r_1 r_2}{\left(r_1+r_2\right)^2+d^2} \tag{1.12}$$

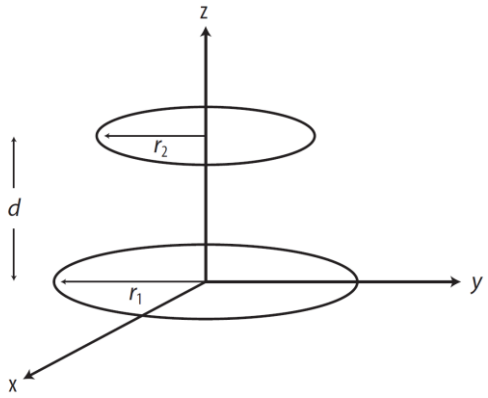


Figure 1-14: Two coils arranged co-axially along a central axis.

## 1.4. Thesis Contribution

This thesis focuses on the fundamental aspects and methodologies to maximize the efficiency of magnetic resonance based WPT systems.

- In reality, due to a resonant coupling nature of the WPT system, for the most efficient power transmission, there is an optimum range between a power coil and a transmitting coil for a fixed distance between the transmitting and receiving coils. This effect may not be clarified by a conventional magnetic induction theory. In this thesis, an equivalent circuit model for a WPT system via magnetic resonance will be derived and analytically solved. From the solution, above effect could be easily clarified and key concepts including frequency splitting and impedance matching will be mentioned as well.

- In addition, methodologies for improving the efficiency of the WPT systems with single, multiple receivers and misalignment condition will be proposed. Theoretical analysis are studied and compared with EM simulation by HFSS and circuit parameters extraction by ADS, as well as experiments, showing agreement with the proposed methodologies.

# Chapter II

# System Model and Circuit Analysis of Magnetic resonance based WPT System

This chapter introduces a system model and circuit analysis of four-coil WPT system. Then, the comparison of different coupling mechanisms is studied and the case of multiple receivers is also mentioned.

## 2.1. System Model and Circuit Analysis

The magnetic resonance (or magnetic resonant coupling) based WPT techniques are typically relied on four coils as opposed to two coils used in the conventional inductive links. A typical model of four-coil power transfer system is shown in Fig. 2-1, which consists of a power coil, a transmitting coil (Tx coil), a receiving coil (Rx coil) and a load coil. The Tx coil and Rx coil are so-called resonators, which are supposed to resonate at the same frequency. For common cases, four coils are different in size. Indeed, in some applications, the coils in the receiver side are needed to be scaled as small enough to be integrated in portable devices such as laptops, handheld devices or implantable medical equipment. In various cases of practical interest, the receiving and load coils can be fitted within the dimensions of those personal assistant tools, enabling mobility and flexibility properties. Otherwise, it is quite free to determine sizes of the transmitter. Normally, the transmitting coil can be made larger for the higher efficiency of the system. For the system in Fig. 2-1, a drawback of a low coupling coefficient between the Tx and Rx coils, as they locate a distance away from each other, is possibly overcome by using high-Q coils. This may help improve the system performance. In other words, the system is able to maintain the high efficiency even when the receiver moves far away from the transmitter. In the transmitting part, a signal generator is used to generate a sinusoidal signal oscillating at the frequency of interest. A power of the output signal from the generator is too small, approximately tens to hundreds of milliwatts, to power devices of tens of watts. Hence, this signal is delivered to the Tx coil through a power amplifier (PA) for signal power amplification. In the receiver side, the receiving resonator and then load coil will transfer the induced energy to a connected load such as a certain electronic device. While the efficiency of the two-coil counterpart is unproportionally dependent on the operating distance, the four-coil system is less sensitive to changes in the distance between the Tx and Rx coils. This kind of system can be optimized to provide a maximum efficiency at the given operating distance. These characteristics will be analyzed in the succeeding sections.

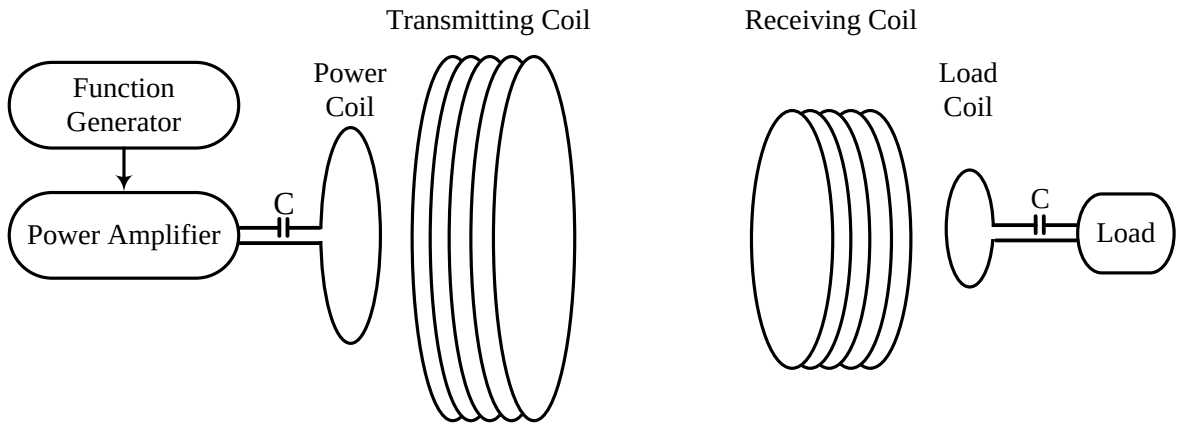


Figure 2-1: Model of four-coil WPT system.

Fig. 2-2 shows the circuit representation of the four-coil system as modeled above. The schematic is composed of four resonant circuits corresponding to the four coils. These coils are connected together via a magnetic field, characterized by coupling coefficients $k_{12}$, $k_{23}$, and $k_{34}$. Because the strengths of cross couplings between the power coil and Rx coil, and the load coil Tx coil are very weak due to utilizing Tx and Rx resonators with multiple of coil turns, they can be neglected in the following analysis. Theoretically, the coupling coefficient (also called coupling factor) has a range from 0 to 1. If all magnetic flux generated from a transmitting coil is able to reach a receiving coil, the coupling coefficient would be "1". On the contrary, the coefficient would be represented as "0" when there is no interaction between them. Actually, there are some factors identifying the coupling coefficient. It is effectively determined by the distance between the coils and their relative sizes. It is additionally determined by shapes of the coils and orientation (angle) between them. The coupling coefficient can be calculated by using a given formula:

$$k_{xy} = \frac{M_{xy}}{\sqrt{L_x L_y}} \tag{2.1}$$

Where $M_{xy}$ is mutual inductance between coil "x" and coil "y" and note that $0 \leq k_{xy} \leq 1$. Referring to the circuit schematic, an AC power source with output impedance of $R_s$ provides energy for the system via the power coil. Normally, the AC power supply can be either a power amplifier or a vector network analyzer (VNA) which is useful to measure a transmission and reflection ratio of the system. Hence, a typical value of $R_S$, known as the output impedance of the power amplifier or the VNA, is 50 $\Omega$. The power coil can be modeled as an inductor $L_1$ with a parasitic resistor $R_1$. A capacitor $C_1$ is added to make the power coil resonate at the desirable frequency. The Tx coil is a helical coil with many turns represented as an inductor $L_2$ with parasitic resistance $R_2$. Geometry of the Tx coil determines its parasitic capacitance such as stray capacitance, which is represented as $C_2$. Since this k-

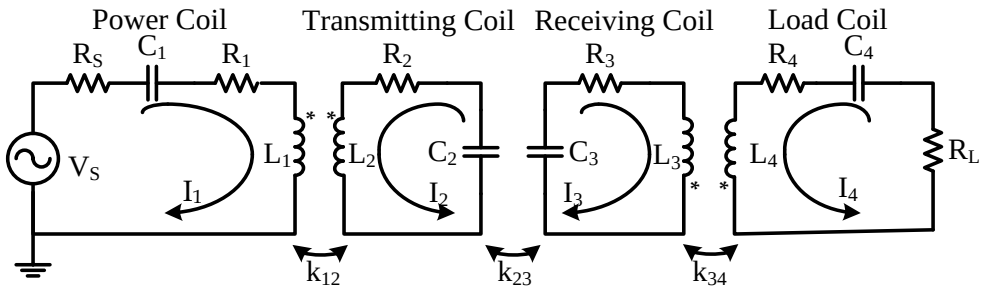


Figure 2-2: Equivalent circuit of four-coil system.

ind of capacitance is difficult to be accurately predicted, for fixed size of the coil, a physical length, which impacts the self-inductance and the parasitic capacitance, has been manually adjusted in order to fit the resonant frequency as desired. In the receiver side, the Rx coil is modeled respectively by $L_3$, $R_3$ and $C_3$. The load coil and the connected load are also performed by $L_4$, $R_4$ and $R_L$. A capacitor $C_4$ also has the same role as $C_1$, so that the resonant frequency of the load coil is defined. When the frequency of sinusoidal voltage source $V_S$ is equal to the self-resonant frequency of the resonators, their impedances are at least. In the other words, currents of the coils would be at the most and energy can be delivered mostly to the receiving coil. Otherwise, energy of the transmitting power source would be dissipated in the power coil circuit itself, resulting in the very low efficiency. In general, setting the frequency of AC supply source as same as the natural resonant frequency of the transceiver coils is one of key points to achieve a higher performance of the system.

As can be seen from Fig. 2-2, the Tx coil is magnetically coupled to the power coil by the coupling coefficient $k_{12}$. In fact, the power coil is one of the forms of impedance matching mechanism. The same situation experiences in the receiving part where the Rx coil and load coil are magnetically linked by $k_{34}$. The strength of interaction between the transmitting and receiving coils is characterized by the coupling coefficient $k_{23}$, which is decided by the distance between these coils, a relative orientation and alignment of them. In general, it is able to use other mechanisms for the impedance matching purpose in either or both sides of the system. For example, a transformer or an impedance matching network, which consists of a set of inductors and capacitors configured to connect the power source and the load to the resonators, is routinely employed. Similar to aspects mentioned above, in reality, the power and Tx coils would be implemented monolithically for the sake of convenience; hence the coupling coefficient $k_{12}$ would be stable. For the same objective, $k_{34}$ would also be fixed. Therefore, there only remains coefficient $k_{23}$ which is so-called an environment variable parameter. The parameter varying with usage conditions, may include the range between the resonator coils, a relative orientation and alignment between them and a variable load on the receiving resonator.

The circuit model offers a convenient way to systematically analyze the characteristic of the system.

By applying circuit theory Kirchhoff‘s Voltage Law (KVL) to this system, with the currents in each resonant circuit chosen as illustrated in Fig. 2-2, a relationship between currents through each coil and the voltage applied to the power coil can be captured as a following matrix:

$$\begin{bmatrix} V_S \\ 0 \\ 0 \\ 0 \end{bmatrix} = \begin{bmatrix} Z_1 & j\omega M_{12} & 0 & 0 \\ j\omega M_{12} & Z_2 & -j\omega M_{23} & 0 \\ 0 & -j\omega M_{23} & Z_3 & j\omega M_{34} \\ 0 & 0 & j\omega M_{34} & Z_4 \end{bmatrix} \begin{bmatrix} I_1 \\ I_2 \\ I_3 \\ I_4 \end{bmatrix} \tag{2.2}$$

Where $Z_1$, $Z_2$, $Z_3$, and $Z_4$ respectively are loop impedances of the four coils. These impedances can be indicated as below:

$$Z_1 = R_S + R_1 + j\left(\omega L_1 - \frac{1}{\omega C_1}\right) \tag{2.3}$$

$$Z_2 = R_2 + j\left(\omega L_2 - \frac{1}{\omega C_2}\right) \tag{2.4}$$

$$Z_3 = R_3 + j\left(\omega L_3 - \frac{1}{\omega C_3}\right) \tag{2.5}$$

$$Z_4 = R_L + R_4 + j\left(\omega L_4 - \frac{1}{\omega C_4}\right) \tag{2.6}$$

From the matrix (2.2), by using the substitution method, the current in the load coil resonant circuit is derived as given:

$$i_4 = -\frac{j\omega^3 M_{12} M_{23} M_{34} V_S}{Z_1 Z_2 Z_3 Z_4 + \omega^2 M_{12}^2 Z_3 Z_4 + \omega^2 M_{23}^2 Z_1 Z_4 + \omega^2 M_{34}^2 Z_1 Z_2 + \omega^4 M_{12}^2 M_{34}^2} \tag{2.7}$$

It is clearly seen that the voltage across the load is equal to $V_L = -I_4 R_L$ and the relationship between the voltages of source and load is given as $V_L/V_S$.

The system model can be considered as a two port network. To analyze a figure of merit of this kind of system, S – parameter is a suitable candidate. Actually, $S_{21}$ is a vector referring to a ratio of signal exiting at an output port to a signal incident at an input port. This parameter is really important because a power gain, the critical factor determining of power transfer efficiency, is given by $|S_{21}|^2$, the squared magnitude of $S_{21}$. The parameter of $S_{21}$ is calculated by [22]:

$$S_{21} = 2\frac{V_L}{V_S}\left(\frac{R_S}{R_L}\right)^{1/2} \tag{2-8}$$

| Transmitter Side | | Receiver Side | |
|---|---|---|---|
| **Parameter** | **Value** | **Parameter** | **Value** |
| **$R_S$** | 50 Ω | $L_3$ | 0.4 μH |
| **$L_1$** | 0.5 μH | $R_3$ | 0.02 Ω |
| **$R_1$** | 0.015 Ω | $C_3$ | 357.5 pF |
| **$C_1$** | 286 pF | $k_{34}$ | 0.1 |
| **$k_{12}$** | 0.05 | $L_4$ | 0.1 μH |
| **$L_2$** | 1.3 μH | $R_4$ | 0.012 Ω |
| **$R_2$** | 0.03 Ω | $C_4$ | 1.43 nF |
| **$C_2$** | 110 pF | $R_L$ | 50 Ω |
| **$k_{23}$** | 0.0001 to 0.3 | frequency | 11-16 MHz |

Table 2-1: Example of practical circuit values.

Thus, combining with $M_{xy} = k_{xy}\sqrt{L_x L_y}$ derived from (1), the $S_{21}$ parameter is given as:

$$S_{21} = \frac{j2\omega^3 k_{12}k_{23}k_{34}L_2L_3\sqrt{L_1L_4R_SR_L}}{Z_1Z_2Z_3Z_4 + k_{12}^2L_1L_2Z_3Z_4\omega^2 + k_{23}^2L_2L_3Z_1Z_4\omega^2 + k_{34}^2L_3L_4Z_1Z_2\omega^2 + k_{12}^2k_{34}^2L_1L_2L_3L_4\omega^4} \quad (2\text{-}9)$$

It is helpful to analyze the performance of the system according to equation (2.9). With all the circuit parameters provided in Table 1, the parameter regarded as the factor determining the efficiency of the system, magnitude of $S_{21}$, can be performed by a function of only two variables $k_{23}$ and frequency. As referred, the coupling coefficient $k_{23}$ is the parameter which varies according to changes in circumstances. A changeable distance, for instance, is a cause of $k_{23}$ variation. In addition, changes in the orientation or misalignment between the transmitting and receiving resonators make the above coefficient inconsistent as well. Actually, when the distance increases, $k_{23}$ will go down because the mutual inductance between those coils declines with distance. In case of a variable orientation or misalignment, the $k_{23}$ also changes. The relation among $|S_{21}|$, $k_{23}$ and frequency is demonstrated in Fig. 2-3. Note that in practice, a vector of $S_{21}$ parameter including magnitude and phase information can be measured by using VNA. From Fig. 2-3, it is clearly seen that when $k_{23}$ is small in cases of the large distance between the transmitter and the receiver or the misalignment, orientation deviation taking place, the efficiency represented as $S_{21}$ magnitude is able to reach a peak at the self resonant frequency of approximately 13.3 MHz. However, the resonant frequency separates as $k_{23}$ is over a certain level. The phenomenon is so-called frequency splitting which has a negative impact on the system efficiency. For instance, as long as the transmitting and receiving coils are such closed as the coupling coefficient $k_{23}$ between them is 0.1, the resonant frequency splits into two peaks at 12.69 and

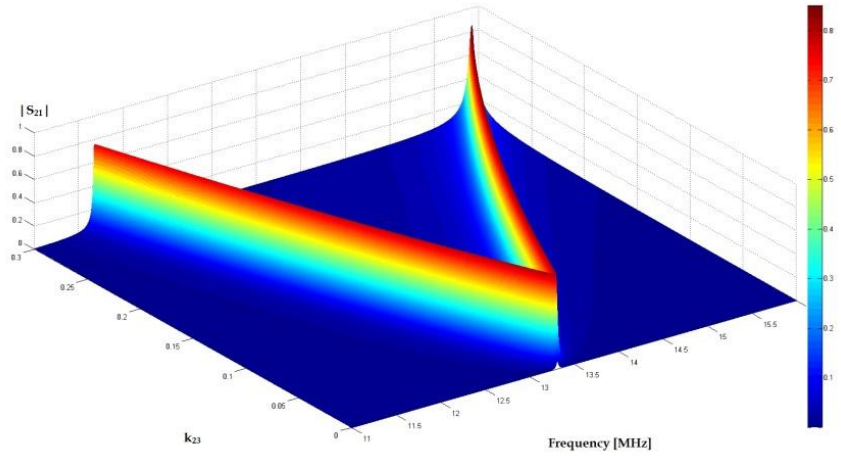


Figure 2-3: $|S_{21}|$ as a function of $k_{23}$ and frequency (3D – View).

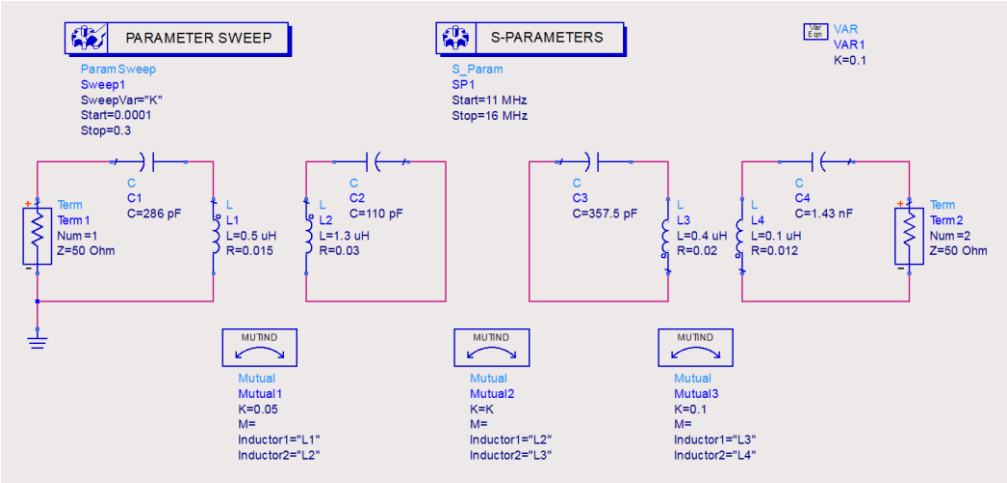


Figure 2-4: Simulation setup using Advanced Design System (ADS).

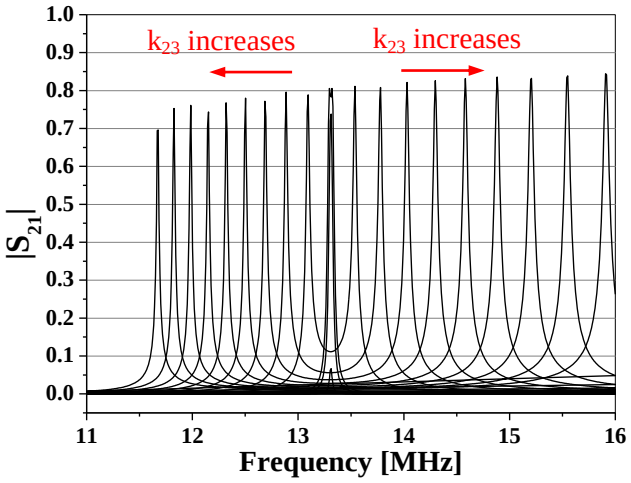


Figure 2-5: Simulation result showing $|S_{21}|$ as a function of $k_{23}$ and frequency (2D – View).

14.03 MHz as observed from Fig. 2-3. Consequently, the system performance is considerably degraded. In order to overcome the drawback, an automatically frequency tuning circuit is needed. The circuit is used to track the resonant frequency of interest so as to preserve the efficiency of the system in cases of transceivers' mobility. It is possible to simulate the system by using Advanced Design System (ADS) of Agilent Technologies. With the circuit setup illustrated in Fig. 2-4, the result of the magnitude of $S_{21}$ can be obtained as shown in Fig. 2-5.

It is instructive to analyze carefully a trend of $|S_{21}|$ as $k_{23}$ variation. Fig. 2-5 clarifies that when the coefficient $k_{23}$ is absolutely small corresponding to a case that the transmitter and the receiver are too far away each other, $|S_{21}|$ is low. When the distance between the resonators is getting closer, $k_{23}$ increases bringing about the higher magnitude of $S_{21}$. However, as $|S_{21}|$ increases to a certain level, the higher $k_{23}$ does not lead to a higher amount of $|S_{21}|$. Moreover, there is the frequency splitting issue which substantially reduces the system efficiency. The point, at which the deviation of the original resonant frequency (13.3 MHz) happens, plays a prominent role in the system. It clarifies the relative position of the resonators that the performance of the system is the highest. If the distance is longer than that range, the efficiency is poorly defined. On the contrary, the resonant frequency detunes along two furrows, but the efficiency is still high. Thus, it would be the maximum power transfer if the frequency can be tuned to the desirable frequency.

Coming back the system equation indicated in (2.9), let expand this equation in terms of quality factor which appreciates how well the resonator can oscillate. The quality factor is presented in a formula as given below:

$$Q_i = \frac{1}{R_i}\sqrt{\frac{L_i}{C_i}} = \frac{\omega_i L_i}{R_i} \Leftrightarrow \omega_i L_i = R_i Q_i \ , i = 1 \sim 4 \tag{2.10}$$

Where $\omega_i$ and $R_i$ are respectively the self-resonant frequency and equivalent resistance of each resonant circuit. In the power coil, for instance, $R_i$ is a sum of $R_S$ and $R_1$. Actually, $\omega_i$ of each coil is defined to be the same, $\omega_1 = \omega_2 = \omega_3 = \omega_4 = \omega_0$. When the resonance takes place, the total impedance of each coil is presented as following:

$$Z_1 = R_S + R_1 \approx R_S \tag{2.11}$$

$$Z_2 = R_2 \tag{2.12}$$

$$Z_3 = R_3 \tag{2.13}$$

$$Z_1 = R_L + R_4 \approx R_L \tag{2.14}$$

For simplicity, in addition to the fact that system parameters can be measured by VNA, it is common to set $R_S$ equal to $R_L$. At the resonant frequency, $\omega_0 = 1/\sqrt{L_i C_i}$, from (2.9), the magnitude of $S_{21}$ can be written as:

$$|S_{21}| = \frac{2k_{12}k_{23}k_{34}Q_2Q_3\sqrt{Q_1Q_4}}{1+k_{12}^2Q_1Q_2+k_{23}^2Q_2Q_3+k_{34}^2Q_3Q_4+k_{12}^2k_{34}^2Q_1Q_2Q_3Q_4} \tag{2.15}$$

As referred previously, the coupling coefficient $k_{12}$ and $k_{34}$ would be constant. There is only $k_{23}$ varying with medium conditions. To find the range between the resonators at which $|S_{21}|$ or the efficiency is certainly at maximum, a derivative of $S_{21}$ with respect to $k_{23}$ is taken and then setting the result to zero, yielding:

$$\frac{d|S_{21}|}{dk_{23}} = 0 \Rightarrow k_{23}^* = \sqrt{\frac{\left(1+k_{12}^2Q_1Q_2\right)\left(1+k_{34}^2Q_3Q_4\right)}{Q_2Q_3}} \tag{2.16}$$

This value of $k_{23}^*$ is equivalent to the maximum range that the transmitter is able to effectively transfer power to the receiver at the given resonant frequency (before the resonant frequency breaking in two peaks). Note that $k_{23}^* \le 1$. With the purpose of finding out the maximum efficiency of the system in terms of $|S_{21}|$, it is feasible to substitute $k_{23}$, which is derived above, into equation (2.15):

$$|S_{21}|_{\max} = \frac{k_{12}k_{34}Q_1Q_4R_L}{k_{23}^*\sqrt{L_1\omega_1L_4\omega_4}} = \frac{k_{12}k_{34}Q_1Q_4R_L}{k_{23}^*\sqrt{L_1L_4}\omega_0} \tag{2.17}$$

It is clear that $|S_{21}|_{\max}$ unproportionally depends on $k_{23}^*$. It means for the sake of a higher efficiency, the extent that the highest efficiency can be achievable is shortened. In order to get a greater value of $|S_{21}|_{\max}$, $k_{23}^*$ is supposed to decrease. From equation (2.16), increasing $Q_2$ and $Q_3$ is able to reduce $k_{23}^*$. In general, making the very high-Q transmitting and receiving coils is very crucial so as to achieve the high transfer performance.

For example, from equation (2.17), with the value given in Table 2-1, the maximum value of magnitude of $S_{21}$ parameter is calculated as follows:

$$\omega_0 = \omega_1 = \frac{1}{\sqrt{L_1C_1}} \approx 83.624\times10^6 \ [rad/s]$$

$$Q_1 = \frac{\omega_0 L_1}{R_S + R_1} \approx 0.84$$

$$Q_2 = \frac{\omega_0 L_2}{R_2} \approx 3623.71$$

$$Q_3 = \frac{\omega_0 L_3}{R_3} \approx 1672.48$$

$$Q_4 = \frac{\omega_0 L_4}{R_L + R_4} \approx 0.17$$

$$k_{23}^{*} = \sqrt{\frac{\left(1 + k_{12}^2 Q_1 Q_2\right)\left(1 + k_{34}^2 Q_3 Q_4\right)}{Q_2 Q_3}} \approx 2.34 \times 10^{-3}$$

$$\left|S_{21}\right|_{\max} = \frac{k_{12} k_{34} Q_1 Q_4 R_L}{k_{23}^{*} \sqrt{L_1 L_4}\, \omega_0} \approx 0.82$$

## 2.2. Comparison between Different Coupling Mechanism Systems in WPT

As mentioned in Section 2.1, the advantage of the four-coil system over the two-coil system is the high efficiency even in far afield condition. Why is that so? To answer this question, it is instructive to study three different coupling mechanism based circuits which are demonstrated in Fig. 2-6. A non-resonant inductive coupling circuit in Fig. 2-6(a) is totally based on the principle of an ordinary transformer. This kind of power transfer also uses primary and secondary coils as similar as transformer, but a striking feature is an exclusion of a high permeability coil. Since an energy transmi-

| **Transmitter Side** | | **Receiver Side** | |
|---|---|---|---|
| **Parameter** | **Value** | **Parameter** | **Value** |
| **$R_S$** | 50 Ω | $L_3$ | 5 µH |
| **$L_1$** | 2 µH | $R_3$ | 0.7 Ω |
| **$R_1$** | 0.4 Ω | $C_3$ | 79.2 pF |
| **$C_1$** | 198 pF | $k_{34}$ | 0.1 |
| **$k_{12}$** | 0.1 | $L_4$ | 1 µH |
| **$L_2$** | 30 µH | $R_4$ | 0.25 Ω |
| **$R_2$** | 2 Ω | $C_4$ | 396 pF |
| **$C_2$** | 13.2 pF | $R_L$ | 50 Ω |
| **$k_{23}$** | 0.001 | frequency | 4 – 12 MHz |

Table 2-2: Example of component values for three circuit models.

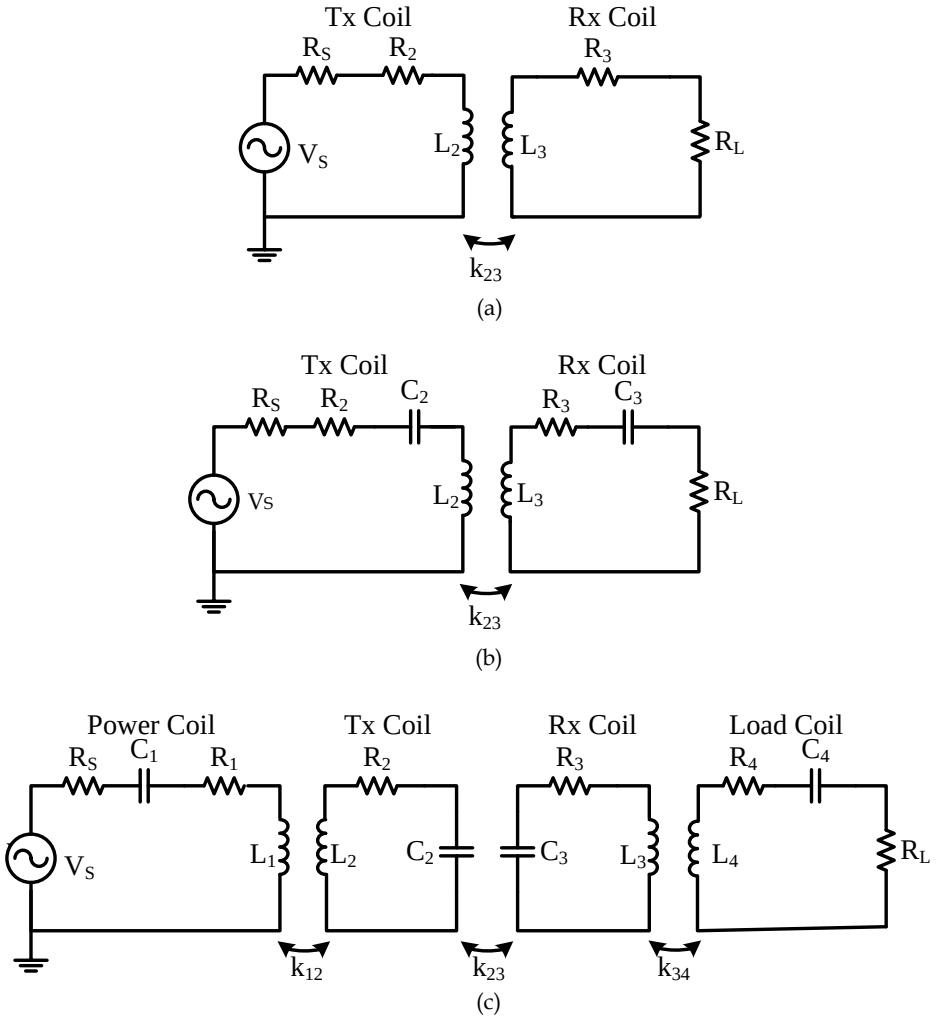


Figure 2-6: Three different coupling mechanism circuits.

(a) Non-resonant inductive coupling based circuit.

(b) Low-Q resonant coupling based circuit (two-coil system).

(c) High-Q resonant coupling based circuit (four-coil system).

ssion is relied on the induction principle, more power is dissipated along the coil or ambient environment and it is more difficult to achieve a long distance transmission.

The above limitation can be overcome using the WPT based on resonant coupling shown in Fig. 2-6(b). By adding external capacitors, coils in primary and secondary side are able to resonate at the same frequency of interest. In fact, high quality factor coils are considered as one of the most critical features for a superior system. In case of Fig. 2-6(b), quality factors of the two resonant circuits are determined by the loading provided by $R_S$ and $R_L$ which are also two major contributors to loss of circuits [23]. Source and load resistances are leading causes of lower Q resonators, deteriorating the s-

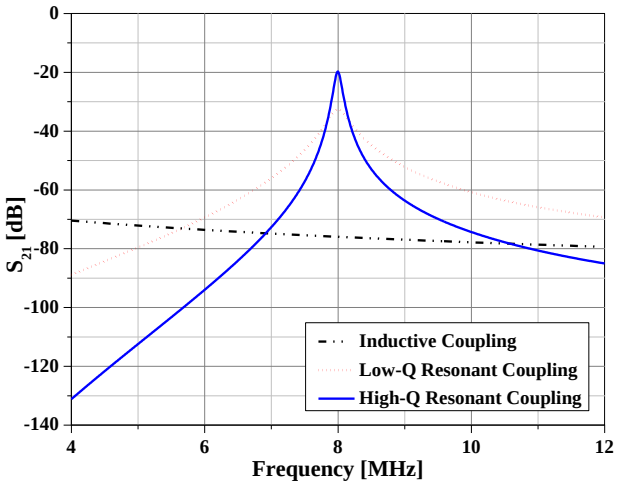


Figure 2-7: Comparison result of three different types of coupling.

ystem efficiency. A solution for this matter is to separate the $R_S$ and $R_L$ from the resonators, that is illustrated in Fig. 2-6(c). Certainly, the resonators have larger quality factors due to the elimination of the unexpected resistances. It is apparent that the quality factors of the transmitting and receiving coils dominantly affect the system performance. In order to comprehend more deeply about the three different circuits, an example with circuit parameters shown in Table 2 is put forward. Fig. 2-7 illustrates a comparison result of the three different coupling methods including inductive coupling, low-Q resonant coupling and high-Q resonant coupling. Note that the two resonant coupling circuits resonate at 8 MHz.

As can be seen, the value of $S_{21}$ in dB is used for the comparison. It is evident that for the inductive coupling mechanism shown in Fig. 2-6(a), the parameter of $S_{21}$ is the lowest. In fact, this value gradually declines from -70 dB to about -80 dB for a frequency range between 4 and 12 MHz. By above analysis, the Q factor of the circuit shown in Fig. 2-6(c) is much greater than that of Fig. 2-6(b). In fact, from Fig. 2-7, $S_{21}$ parameter of the high-Q circuit is approximately 20 dB higher than that of the low-Q circuit. That completely proves the theoretical presumption.

## 2.3. WPT to Multiple Devices through Resonant Coupling

All the approaches mentioned previously are merely in terms of one to one WPT. That means one transmitter, which includes a power coil and a transmitting coil, provides energy wirelessly to only one receiver consisting of receiving and load coils in a distance away. In reality, however, the cases of multiple small receivers are in favor and needed to be considered carefully. Transferring power to a couple of receivers is also based on the same principle as one to one case. Nevertheless, an effect of two receivers in proximity is considerable. Thus, several cases of multiple receivers wireless energy transmission will be investigated. In case of two identical receivers located sufficiently far field and t-

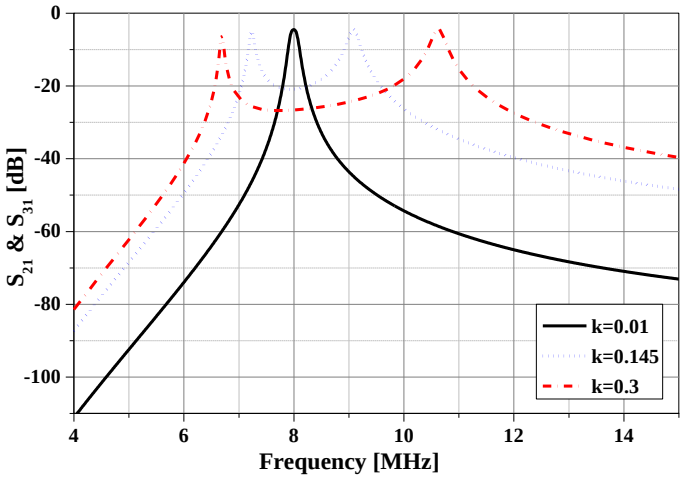


Figure 2-8: Performance of two identical receivers in case of no interaction between them.

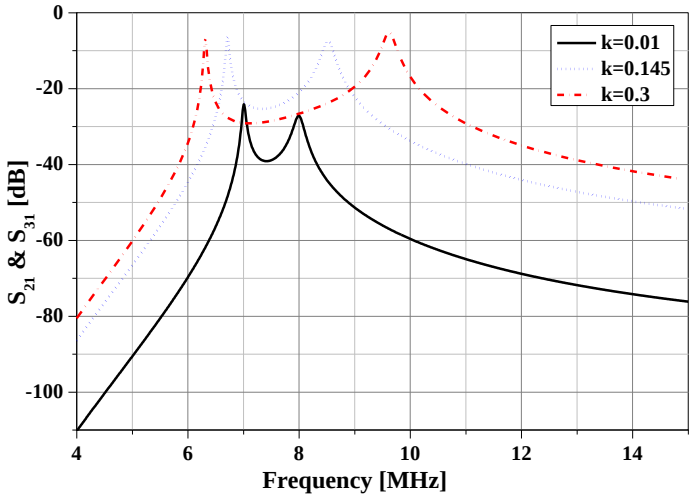


Figure 2-9: Performance of two identical receivers in case of strong interaction.

here is no interaction between them, the system can be interpreted as a sum of two discrete systems.

Since the two receivers are identical, their operations are coincident with each other if they experience a same condition such as the strength of coupling. With the circuit parameters shown in Table 2, only difference in the coupling coefficient between the transmitting and receiving coils, the performance of the two receivers is illustrated in Fig. 8. It is undoubtedly true that the resonant frequency splits into two peaks as an increase of k, which is the coupling coefficient between the two receivers and the transmitter. The stronger the coupling is, the more the new resonant frequencies deviate from the original resonant frequency. At k of 0.01, for example, the system efficiency hits the peak at 8 MHz. When the coupling getting stronger to 0.145 and then 0.3, the original peak respectively breaks in two other peaks at about 7.2 and 9.1 MHz; 6.7 and 10.6 MHz. On the other hand, as shown in Fig. 9, in case of the strong interaction between receiving coils, even at low k, the resonant frequency is splitted to two peaks at 7 and 8 MHz. When k reaches 0.145, the maximum

power transfer occurs at the frequency of 6.7 and 8.5 MHz. The separation among splitted frequencies is larger at the stronger coupling between the transmitter and the receivers, 6.3 and 9.6 MHz. For a situation that the two receivers resonate at the same frequency but their physical parameters are different, the system transfer efficiency is relatively similar. Theoretically, the four circuit model equations derived from the matrix equation (2.2) can be extended for multiple receivers. For one to two system, in particular, the extension of circuit equations is straightforward, with six equations instead of four. By using these equations, it is possible to predict the characteristic of the system with multiple receivers.

# Chapter III

# Adaptive Methods for Efficiency Improvement in Magnetic Resonance based WPT system

This chapter studies several methods to maximize the efficiency of WPT systems with single receiver, multiple receivers and axial-misalignment case.

## 3.1. Efficiency Improvement for Magnetic Resonance based WPT system with Single Receiver

### 3.1.1. Introduction

Medium-range WPT relied on magnetic resonance is a growing research area that finds wide applications. It is clear that the larger sizes of transceivers, the higher efficiency of the system. However, there exists a drawback of low efficiency due to varied distance and small size receiver, in case of applications for mobile consumer electronics. The concept of using coupling between asymmetric resonators with different sizes was proposed in [27]. Nonetheless, no optimization method and theoretical analysis were reported. Since the technique in [28] seems to be impractically applied in consumer electronics, in this section, a model and an equivalent circuit of WPT system are introduced, and an adaptive method to optimize the system with respect to distance variations is presented. Simulation and experimental results are shown to clarify the analysis.

### 3.1.2. Theoretical Analysis

A schematic of the WPT system for future portable consumer electronics devices is illustrated in Fig. 3-1, which consists of four one-turn loop coils, a power coil, a transmitting coil (Tx coil), a receiving coil (Rx coil) and a load coil. The Tx and Rx coils are also called resonators, which are supposed to resonate at the same frequency. As mentioned, the coils in the receiver side are needed to be scaled and supposed to be planar-sized for integration in handheld devices. Otherwise, it is quite free to determine sizes of the transmitter. $D_1$ is the distance between two coils in the transmitting part. $D_2$, which is the distance between the Tx coil and the coils in receiving side, is considered as the distance for power transfer. Fig. 3-2 illustrates an equivalent circuit representation of the model. The four coils are connected together via a magnetic field, characterized $M_{xy}$ which shows the mutual inductance between the $x$-th and the $y$-th coil. Each coil is represented by lumped components $R$, $L$ an-

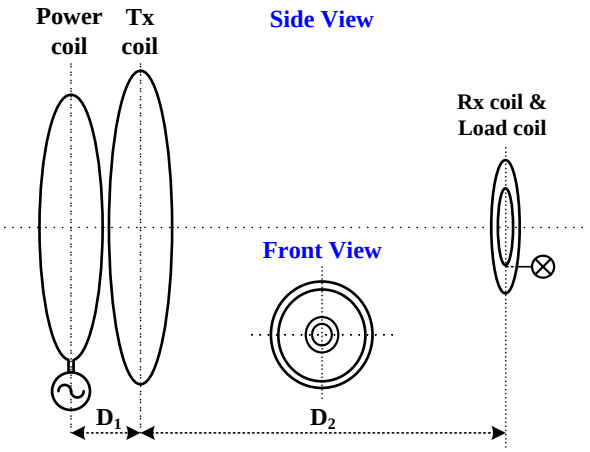


Figure 3-1: Schematic of WPT system with single receiver.

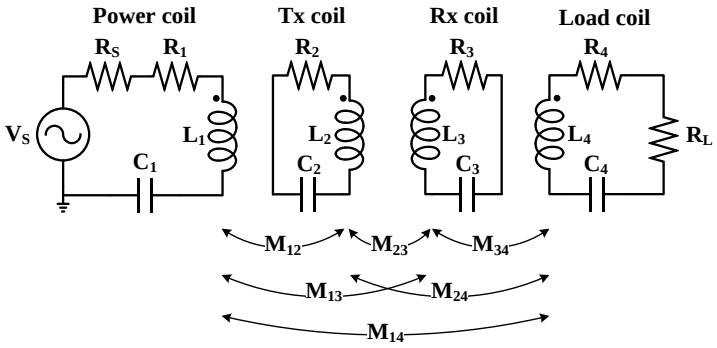


Figure 3-2: Equivalent circuit of the WPT system.

d C. By ap-plying the circuit theory, a relationship between currents through each coil and a voltage source $V_S$ is obtained in the matrix below:

$$\begin{bmatrix} V_S \\ 0 \\ 0 \\ 0 \end{bmatrix} = \begin{bmatrix} Z_1 & j\omega M_{12} & -j\omega M_{13} & -j\omega M_{14} \\ j\omega M_{12} & Z_2 & -j\omega M_{23} & -j\omega M_{24} \\ -j\omega M_{13} & -j\omega M_{23} & Z_3 & j\omega M_{34} \\ -j\omega M_{14} & -j\omega M_{24} & j\omega M_{34} & Z_4 \end{bmatrix} \begin{bmatrix} I_1 \\ I_2 \\ I_3 \\ I_4 \end{bmatrix} \tag{3.1}$$

Where $Z_1$, $Z_2$, $Z_3$, $Z_4$ are the impedance in each loop as mentioned in (2.3) to (2.6) The closed form equation for the mutual inductance $M_{xy}$ of two circular coils with parallel axes has been derived in [20]. Fig. 3-3 shows all relevant variables for calculations. From (1.8), the mutual inductance $M_{xy}$ between the two coils in Fig. 3-3, one with radius $r_x$, and the other with radius $r_y$, with a distance $d$ between their axes and a distance $c$ between plans of the coils, can be calculated as below:

$$M_{xy} = \frac{\mu_0}{\pi}\sqrt{r_x r_y}\int_0^{\pi} \frac{\left[1-\frac{c}{r_y}\cos\phi\right]\Psi(k)}{\sqrt{V^3}}\,d\phi \tag{3.2}$$

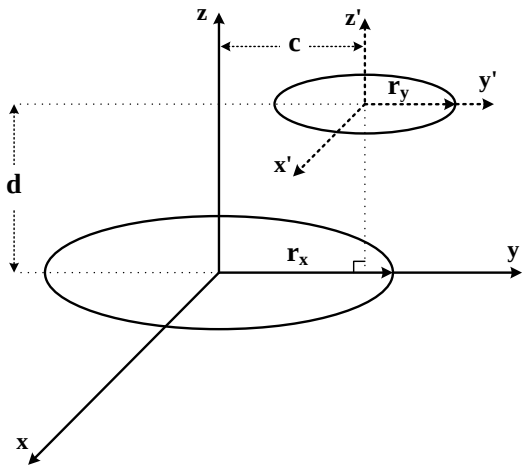


Figure 3-3: Two coils in parallel axes with variables defined for all positions.

### 3.1.3. Proposed Adaptive Method

When the receiver is in close proximity enough with the transmitter, the frequency splitting would occur, causing a considerable decrease in the system performance. Fig. 3-4 illustrates a theoretical plot of $S_{21}$ parameter as a function of $D_1$ and $D_2$, originating from the above circuit derivations with all the mutual couplings being taken into account. As can be seen, when the $D_2$ between the transmitter and the receiver varies, there would be corresponding changes in an optimum value of $D_1$ in order for the power transfer efficiency denoted by $S_{21}$ parameter to be maximized. Based on that analysis, in th-

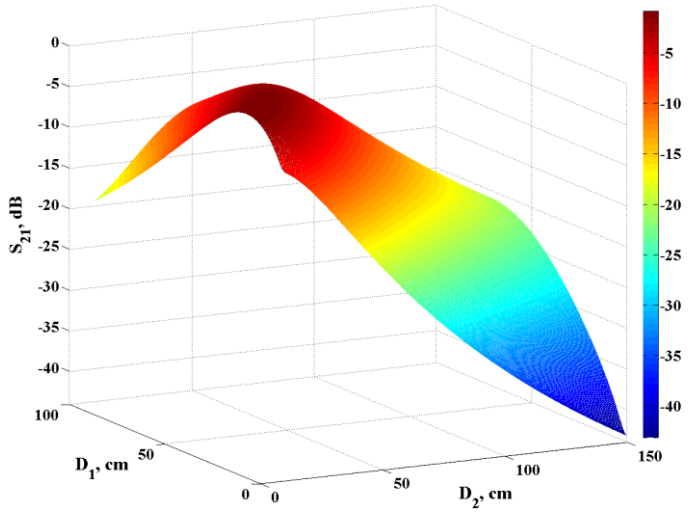


Figure 3-4: $S_{21}$ as a function of $D_1$ and $D_2$ (transmitting side: power coil radius = 32 cm, Tx coil radius 35 cm, receiving side: two identical Rx coils radius = 9 cm, two identical load coils radius = 6 cm). The resonant frequency is set at 10 MHz.

is thesis, a novel method of implementing an optimum distance adaptation '$D_1$', according to the distance variation between the transmitter and the receivers '$D_2$', in the transmitting side enables the system of WPT to multiple receivers with higher efficiency is proposed.

### 3.1.4. Results

The above analysis has been verified by Advanced Design System (ADS) and ANSYS HFSS, in addition to experiment implementation. Initially, only one power coil in the transmitting side is used for verification. Fig. 3-5 shows a one-turn loop coil with 32 cm of radius and copper wire thickness of 6 mm in an experimental shape (left) and HFSS model (right). The Agilent Technologies 8751A vector network analyzer (VNA) was used to measure the $S_{11}$ parameter of the coil. Fig. 3-6 and 3-7 s-

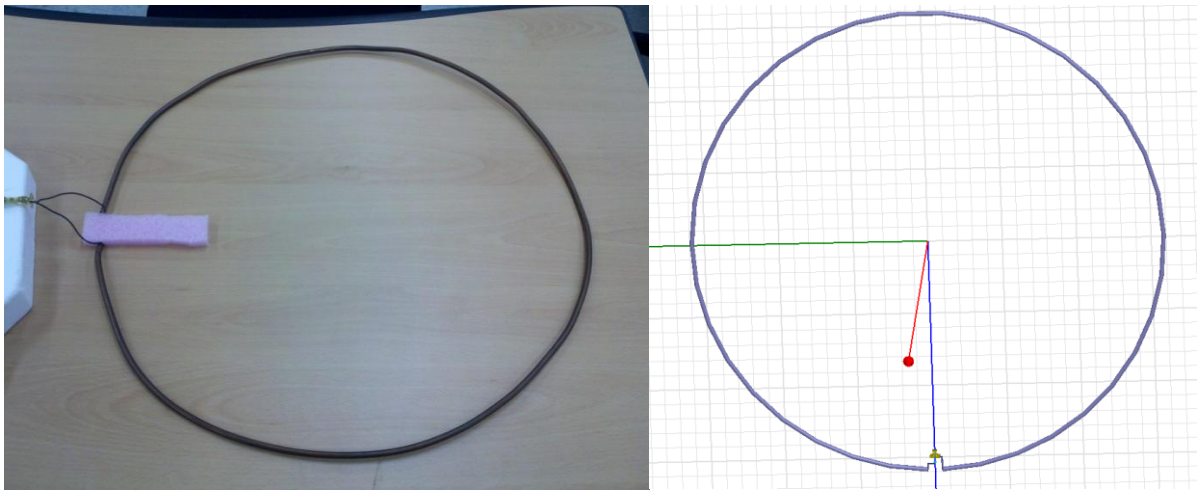

Figure 3-5: One-turn loop coil with radius of 32 cm in experimental shape and HFSS model.

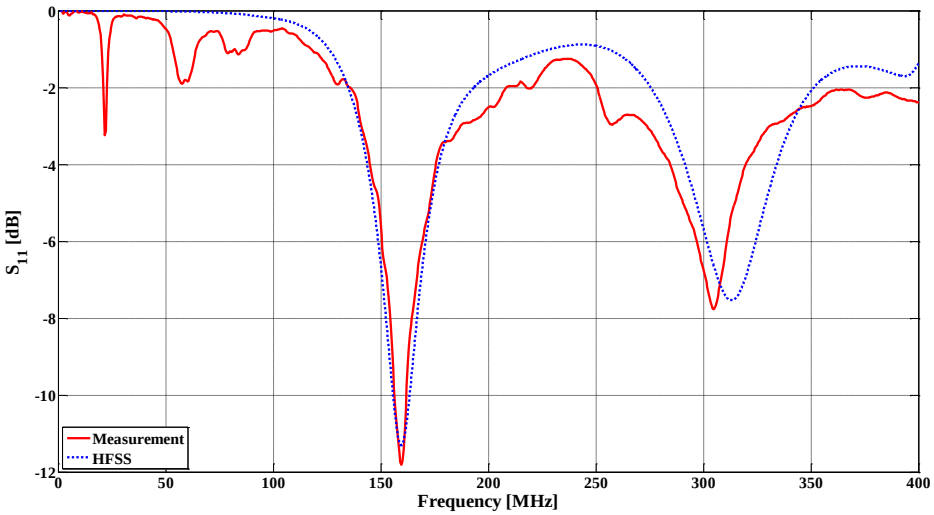


Figure 3-6: Comparison of measured and simulated $S_{11}$ of one-turn loop coil with radius of 32 cm.

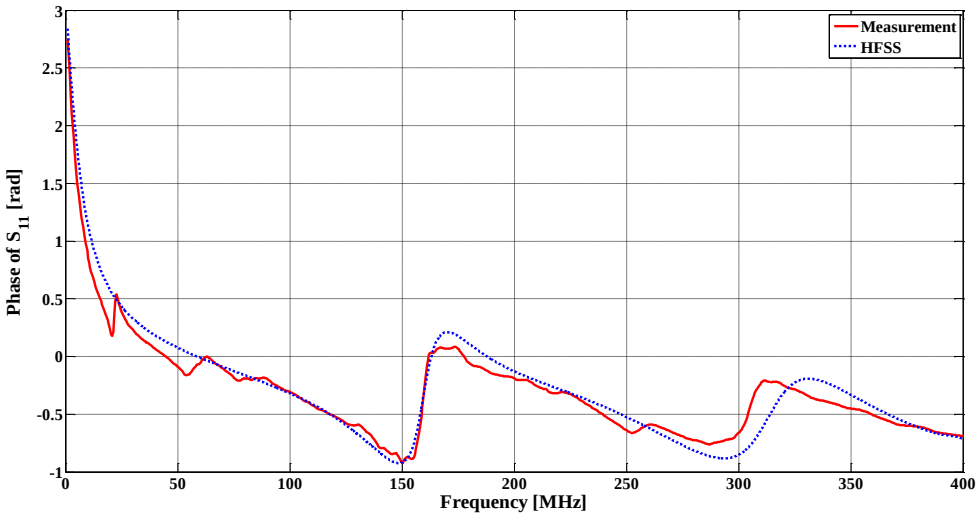


Figure 3-7: Comparison of measured and simulated phase of $S_{11}$ of one-turn loop coil with radius of 32 cm.

hows the comparison of the magnitude and phase of S11 parameter between experiment and EM simulation in HFSS. It is shown a good agreement between experimental results and results getting from HFSS simulation. Then, the WPT system model in HFSS and its circuit extraction were also verified. The model specification of the WPT system described in Fig. 3-4 was utilized. The system model in HFSS was shown in Fig. 3-8 and Fig. 3-9 shows the circuit extraction of lumped components R, L and C of the above model in ADS. At the distance $D_1$ of 5 cm and $D_2$ of 20 cm, the

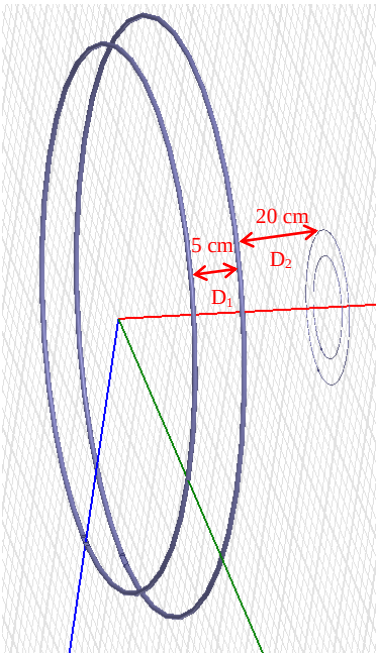


Figure 3-8: WPT system model in HFSS.

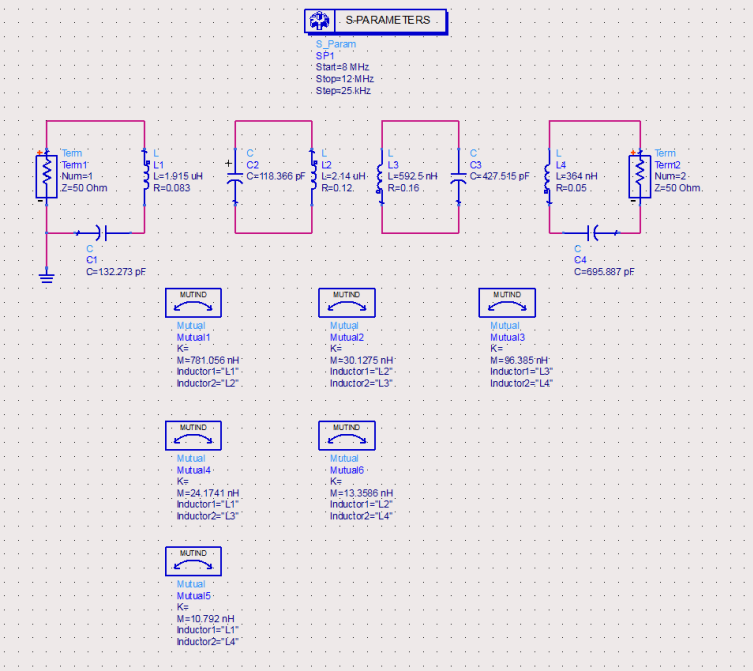


Figure 3-9: Circuit extraction of the above WPT system model in ADS.

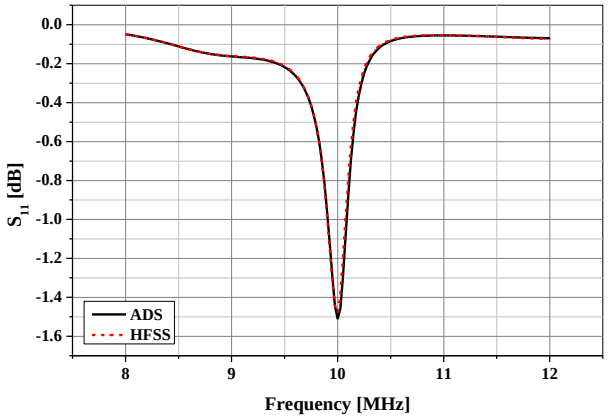


Figure 3-10: Circuit extraction of the above WPT system model in ADS.

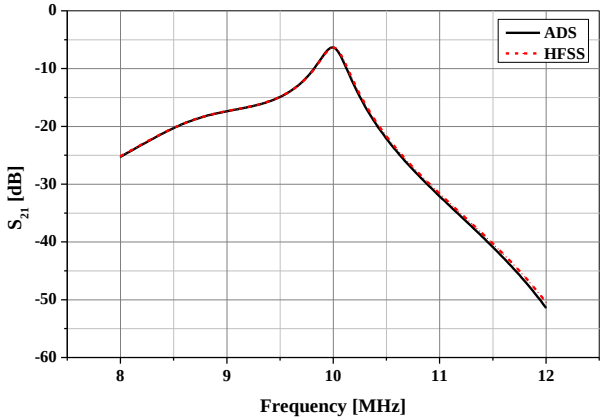


Figure 3-11: Circuit extraction of the above WPT system model in ADS.

simulated $S_{11}$ and $S_{21}$ parameter by both ADS and HFSS. After the process of the system verification, the proposed method was validated by comparing the WPT system with and without using the adaptive method. The simulated results are plotted in Fig. 3-12, showing the better performance by using the adaptive method. Additionally, the experimental implementation was also done to verify the effectiveness of the proposed method. The experimental setup is shown in Fig. 3-13. All the coils were made of one-turn loops. In the transmitting side, the power coil and Tx coil were with 32 cm and 34 cm of radius, respectively. These two coils were made by 6 mm diameter copper wire. In the receiving side, the two identical pairs of the Rx and load coils were designed with 10 cm and 5 cm of

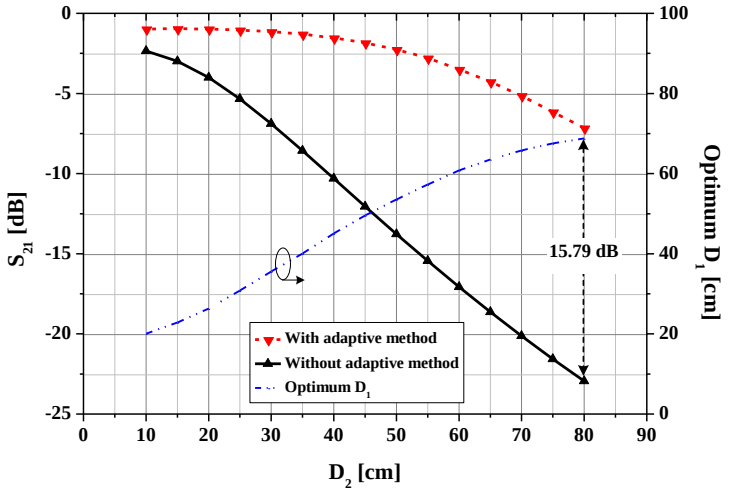


Figure 3-12: Simulated $S_{21}$ parameter comparison between the system with and without the adaptive method. In case of without adaptive method, the $D_1$ was fixed at 10 cm.

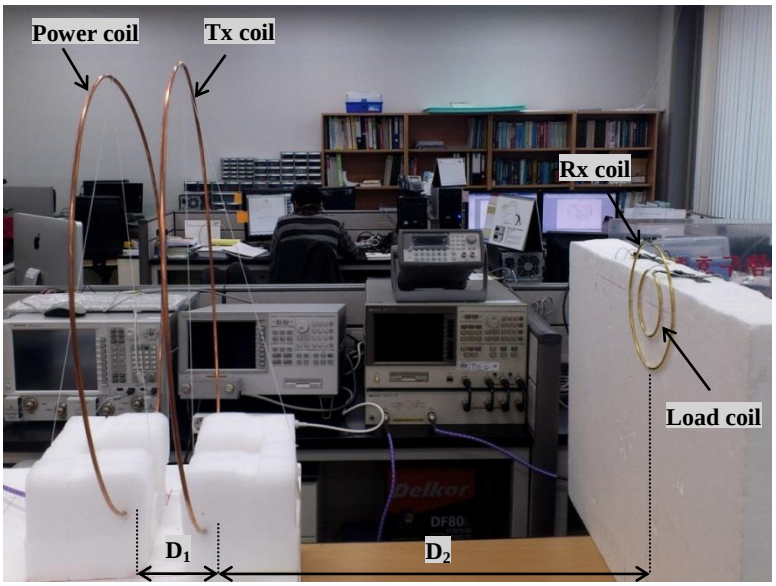


Figure 3-13: Experimental setup of the WPT system with single receiver.

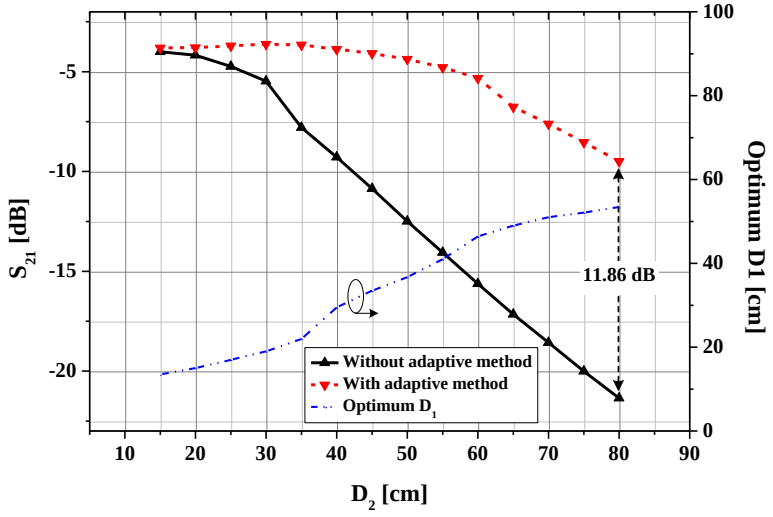


Figure 3-14: Measured $S_{21}$ parameter comparison between the system with and without the adaptive method. In case of without adaptive method, the $D_1$ was fixed at 10 cm.

radius and copper wire thickness of 4 mm. The Rx and load coils of each pair are concentrically located. Variable capacitors were added in the transmitter and receivers to set the resonant frequency of interest. The measured resonant frequency of the implemented system was 10 MHz. The $S_{21}$ parameter was measured by Agilent Technologies 8751A vector network analyzer (VNA) and examined every 5 cm from 15 to 80 cm. The experimental results are plotted in Fig. 3-14 shows a 11.86 dB boost in $S_{21}$ parameter at the distance $D_2$ of 80 cm.

## 3.2. Efficiency Improvement for Magnetic Resonance based WPT with Multiple Receivers

### 3.2.1. Introduction

A novel method using a magnetic resonant technology was proposed in [3], in which only single receiver was considered. Of considerable interest for practical application to the magnetic resonance based WPT systems is the case of multiple receivers. In chapter 2 and [23], the case of multiple receivers with strong coupling interaction was studied, showing the significant degradation in the power transfer efficiency due to a phenomenon of frequency splitting; however no optimization method and theoretical analysis were reported. In this section, an adaptive method to improve the efficiency of the WPT system with multiple receivers is proposed and verified by experimental results.

### 3.2.2. Theoretical Analysis

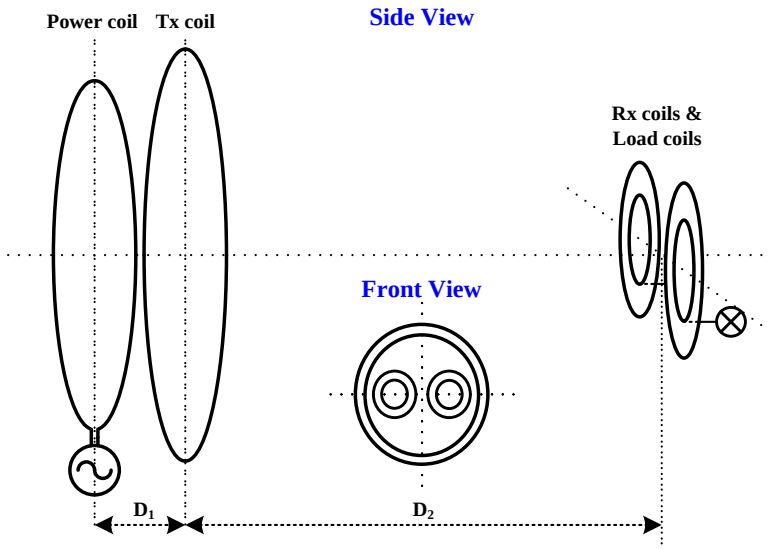


Figure 3-15: Schematic of WPT system with multiple receivers.

A photograph of the system of WPT to multiple receivers is illustrated in Fig. 3-15, which consists of six one-turn loop coils, a power coil and a Tx coil in the transmitting side, and two identical Rx and load coil pairs in the receiving part. The Tx coil and Rx coils are also called resonators, which are supposed to resonate at the same frequency. The two receivers are placed closely on the same plane, where the Rx and load coils of each pair are concentrically located for integration purpose. $D_1$ is the distance between two coils in the transmitting part. $D_2$, which is the distance between the Tx coil and the coils in receiving side, is considered as the distance for power transfer. Fig. 2 illustrates an equivalent circuit representation of the system shown in Fig. 3-15. The six coils are connected together via a magnetic field, characterized by $M_{xy}$ which shows the mutual inductance between the $x$-th and the $y$-th coil. Each coil is represented by lumped components $R$, $L$ and $C$. By applying Kirchhoff's voltage law around each of the six loop coils, a relationship between currents through each coil and a voltage source $V_S$ is obtained at a resonant frequency $\omega$ in the following matrix:

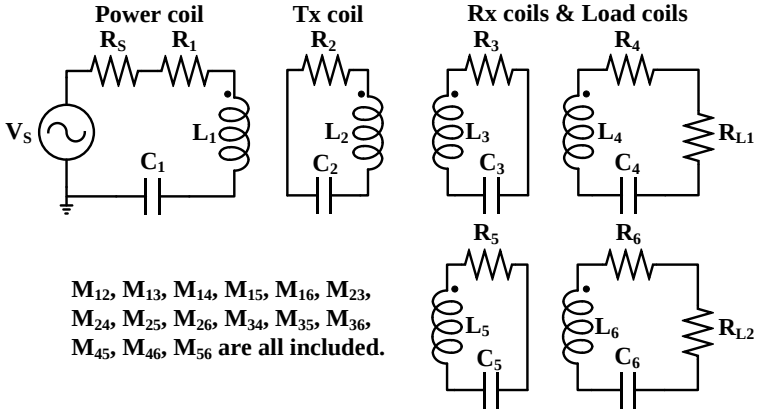


Figure 3-16: Equivalent circuit of WPT system with multiple receivers.

$$\begin{bmatrix} V_S \\ 0 \\ 0 \\ 0 \\ 0 \\ 0 \end{bmatrix} = \begin{bmatrix} Z_1 & j\omega M_{12} & -j\omega M_{13} & -j\omega M_{14} & -j\omega M_{15} & -j\omega M_{16} \\ j\omega M_{12} & Z_2 & -j\omega M_{23} & -j\omega M_{24} & -j\omega M_{25} & -j\omega M_{26} \\ -j\omega M_{13} & -j\omega M_{23} & Z_3 & j\omega M_{34} & j\omega M_{35} & j\omega M_{36} \\ -j\omega M_{14} & -j\omega M_{24} & j\omega M_{34} & Z_4 & j\omega M_{45} & j\omega M_{46} \\ -j\omega M_{15} & -j\omega M_{25} & j\omega M_{35} & j\omega M_{45} & Z_5 & j\omega M_{56} \\ -j\omega M_{16} & -j\omega M_{26} & j\omega M_{36} & j\omega M_{46} & j\omega M_{56} & Z_6 \end{bmatrix} \begin{bmatrix} I_1 \\ I_2 \\ I_3 \\ I_4 \\ I_5 \\ I_6 \end{bmatrix} \tag{3.3}$$

Where $Z_1$, $Z_2$, $Z_3$, $Z_4$, $Z_5$, $Z_6$ are the impedance of each resonant coil. The closed form equation for the mutual inductance $M_{xy}$ of two circular coils with parallel axes was shown in (3.2).

### 3.2.3. Proposed Adaptive Method

When the two receivers are in close proximity, the frequency splitting would occur, causing a considerable decrease in the system performance. Fig. 3-17 illustrates a theoretical plot of $S_{21}$ parameter as a function of $D_1$ and $D_2$, originating from the above circuit derivations with all the mutual couplings being taken into account. As can be seen, when the $D_2$ between the transmitter and the receivers varies, there would be corresponding changes in an optimum value of $D_1$ in order for the power transfer efficiency denoted by $S_{21}$ parameter to be maximized. Based on that analysis, in this thesis, a novel method of implementing an optimum distance adaptation '$D_1$', according to the distance variation between the transmitter and the receivers '$D_2$', in the transmitting side enables the system of WPT to multiple receivers with higher efficiency is proposed.

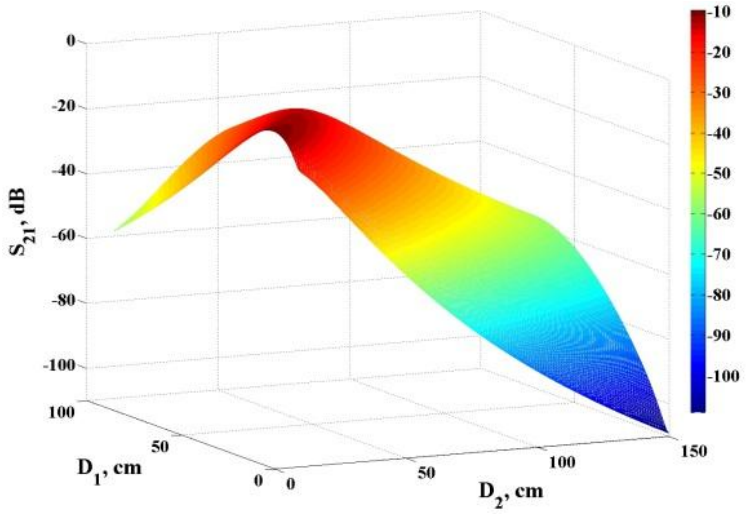


Figure 3-17: $S_{21}$ as a function of $D_1$ and $D_2$ (transmitting side: power coil radius = 32 cm, Tx coil radius = 35 cm, receiving side: two identical Rx coils radius = 9 cm, two identical load coils radius = 6 cm). The two receivers are fixedly placed on the same plane with a separation of 2 cm. The resonant frequency is set at 10 MHz.

## 3.2.4. Results

The model specification of the WPT system described in Fig. 3-4 was utilized, the difference is only the duplicate of receiver. The simulated results are plotted in Fig. 3-18, showing the effectiveness of the propose method. The above optimization method for WPT systems was additionally verified by experimental implementation. All the coils were made of one-turn loops. In the transmitting side, the power coil and Tx coil were with 32 cm and 34 cm of radius, respectively. These two coils were made by 6 mm diameter copper wire. In the receiving side, the two identical pairs of the Rx and load coils were designed with 10 cm and 5 cm of radius and wire thickness of 4 mm. The Rx and load coils of each pair are concentrically located. The two receivers are fixedly attached on the same plane with a separation of 2 cm, which is a gap between the two Rx coils. Variable capacitors were added in the transmitter and receivers to set the resonant frequency of interest. The measured resonant frequency of the implemented system was 10 MHz. The $S_{21}$ parameter was measured by Agilent Technologies 8751A vector network analyzer (VNA) and examined every 5 cm from 15 to 80 cm. The experiment was carried out to evaluate the system efficiency in two cases, with and without the proposed adaptive method. In case of not using the adaptive method, the distance between the two coils in the transmitting side $D_1$ was fixed at 10 cm. On the other hand, the $D_1$ was varied to find out the optimum values, where the $S_{21}$ parameters were at maximum. The experimental setup is shown in Fig. 3-19 and the experimental results are plotted in Fig. 3-20, which presents the measured $S_{21}$ parameter between the transmitter and one of the two receivers, shows a better performance when using the adaptive method. The $S_{21}$ parameter is boosted 12.16 dB at the distance $D_2$ of 80 cm. The measured value of $S_{21}$ of the proposed system is approximately quadruple than a system without the proposed method.

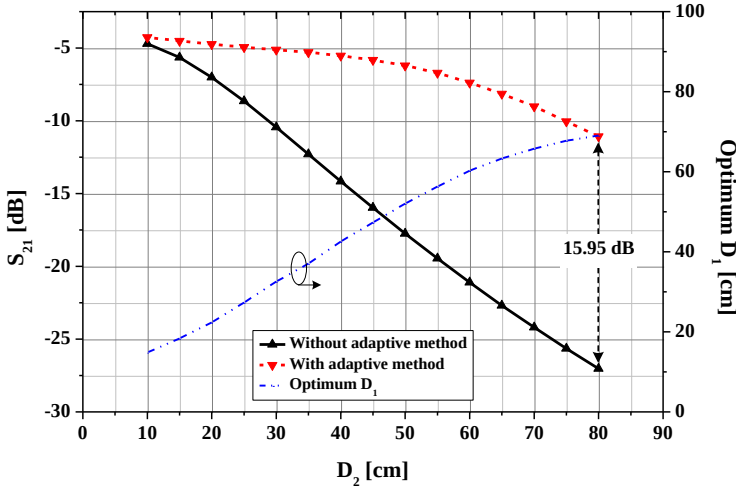


Figure 3-18: Simulated $S_{21}$ parameter comparison between the system with and without the adaptive method. In case of without adaptive method, the $D_1$ was fixed at 10 cm.

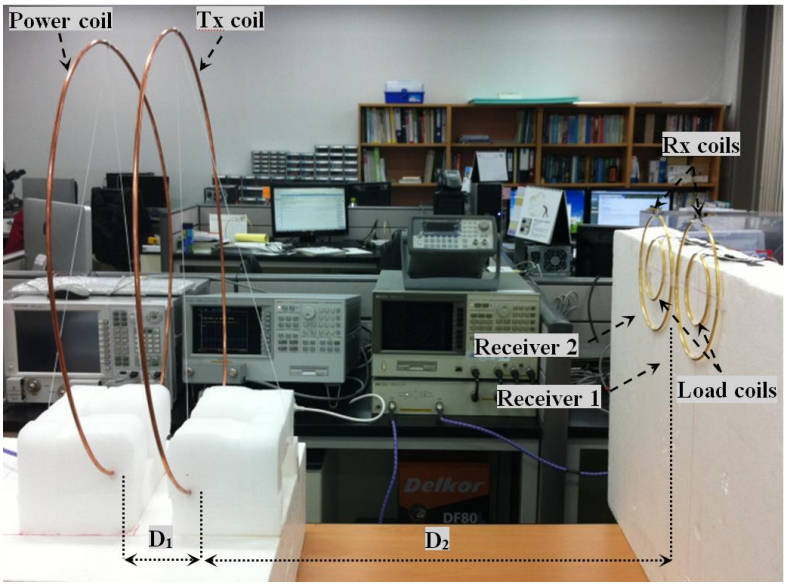


Figure 3-19: Experimental setup of the WPT system with multiple receivers.

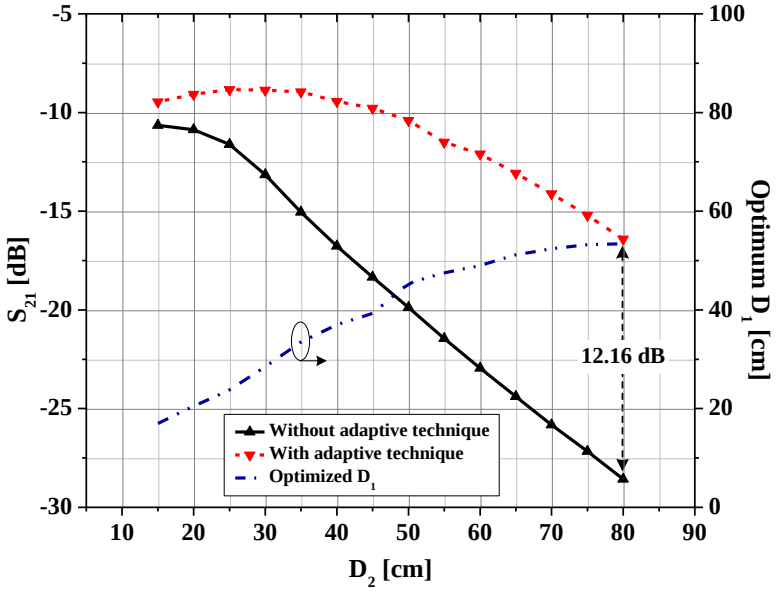


Figure 3-20: Measured $S_{21}$ parameter comparison between the system with and without the adaptive method. In case of without adaptive method, the $D_1$ was fixed at 10 cm.

## 3.3. Efficiency Improvement for Magnetic Resonance based WPT with Axial-misalignment

### 3.3.1. Introduction

In [3], a novel way of transmitting power wirelessly using magnetic resonance was proposed, in which the optimal efficiency results were shown when two resonant devices were perfectly aligned. However, in order to build up a practical wireless power transmission system, axially misalignment case needs to be considered as well. In this section, an adaptive method to improve the system performance in axial-misalignment condition is described. Experimental results are demonstrated to verify the effectiveness of the proposed method.

### 3.3.2. Theoretical Analysis

In the system shown in Fig. 3-21, large coils that are modeled by $L_1$ and $L_2$ are connected together via a magnetic field, characterized by a mutual inductance M. The coils of $L_1$ and $L_2$ form the resonators that resonate at the frequency of interest. The efficiency of WPT system can be modeled with mutual inductance and parasitic resistances; and can be described as follows [29]:

$$\eta = \frac{\omega^2 M^2 R_L}{R_1 (R_2 + R_L)^2 + \omega^2 M^2 (R_2 + R_L)} \tag{3.4}$$

Where $\omega$ is the resonant frequency of the system; $R_1$, $R_2$ are the parasitic resistances of coil $L_1$ and $L_2$ respectively and $R_L$ is the load resistance. A VNA is used to measure the transmission and reflection ratio of the system, where load resistance, $R_L$ is 50 ohm.

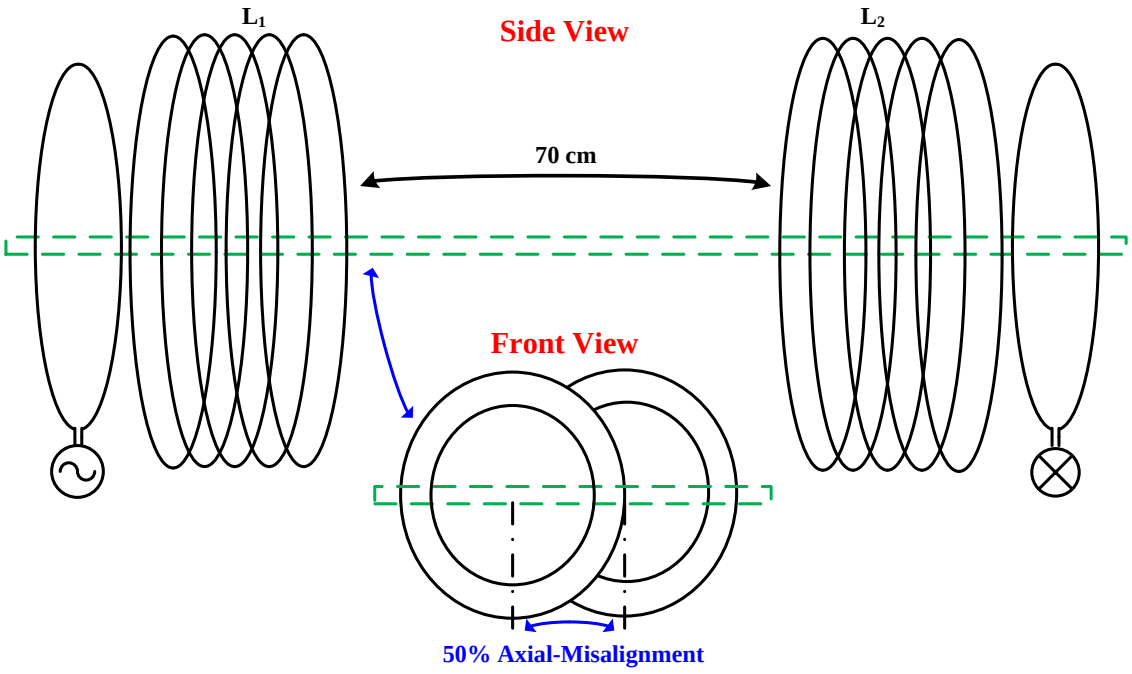


Figure 3-21: Illustration of WPT and experimental environment.

### 3.3.3. Proposed Adaptive Method

Impedance matching has commonly been used as a useful technique to improve the efficiency in wireless communication system [30]. In the case of axial misalignment between two coils of a WPT system, the reflected power would increase causing significant decrease in WPT system performance. In this letter, a novel method of implementing impedance matching in the transmitting side in order to reduce the reflected power enabling WPT system with higher efficiency is proposed in Fig. 3-22 Source impedance and load impedance are described in (3.5). In this case, the transferred power P can be presented as (3.6)

$$Z_{source} = R_{source} + jX_{source} \quad and \quad Z_{load} = R_{load} + jX_{load} \tag{3.5}$$

$$P = \frac{1}{2}|V|^2 \frac{R_{load}}{\left(R_{load} + R_{source}\right)^2 + \left(X_{load} + X_{source}\right)^2} \tag{3.6}$$

And when the mismatch between source impedance and load impedance is eliminated, the power transfer in the WPT system can be described as (3.7):

$$P = \frac{1}{2}|V|^2 \frac{1}{4R_{source}} \tag{3.7}$$

The proposed technique to increase the power transfer performance is implemented with impedance matching circuit in the case with axial misalignment of magnetic resonance WPT system

.

### 3.3.4. Results

The above optimization technique for WPT system with axial misalignment was verified by Avanc-

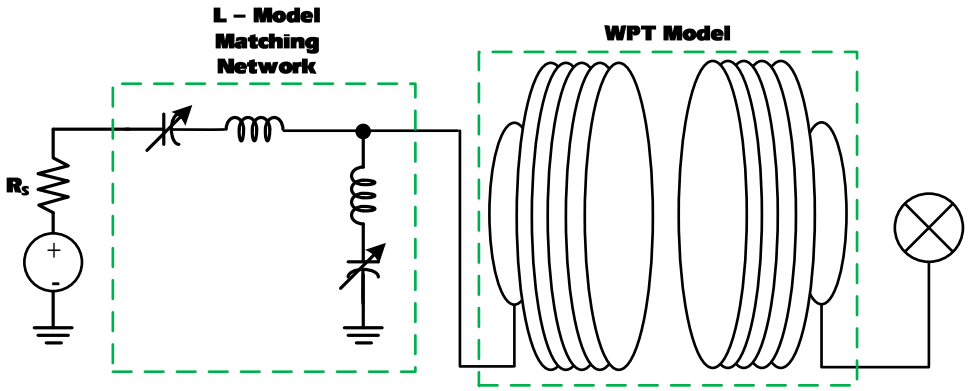


Figure 3-22: Block diagram of the L-model matching network in WPT system.

ed Design System (ADS) and EMPro, in addition to experimental implementation using the model by [3]. The system consists of a power coil, a transmitting coil (Tx coil), a receiving coil (Rx coil) and a load coil. The Tx and Rx coil, also known as the resonators, are designed to resonate at the same frequency. The transmitting side is consisted of a power coil with 49 cm of diameter and the Tx coil that is a helical type with 60 cm diameter and 5.25 turns. Symmetric structure is duplicated on the receiving side for the load coil and Rx coil. These four coils were implemented with a 6 mm diameter copper wire coated with gold and separated by a gap of 4 cm. The measured resonant frequency of the implemented system was 10.14MHz. As can be seen in Fig. 3-21, the distance between the two resonators was set at 70cm and intentionally introduced an axial misalignment by 50% that is equivalent to 35 cm axial separation. Agilent Technologies 8751A VNA is used for the $S_{21}$ parameter measurement. Without the proposed matching circuits, the measured $S_{21}$ is -4.1 dB. With the proposed impedance matching circuit in WPT system, $S_{21}$ parameter reflecting the efficiency in the WPT link is increased by 1.5 dB to -2.9 dB. This measurement result corresponds to 11.4 % improvement in $S_{21}$, or 48.4 % of relative efficiency improvement compared to a WPT link without the proposed matching circuits, Fig. 3-23.

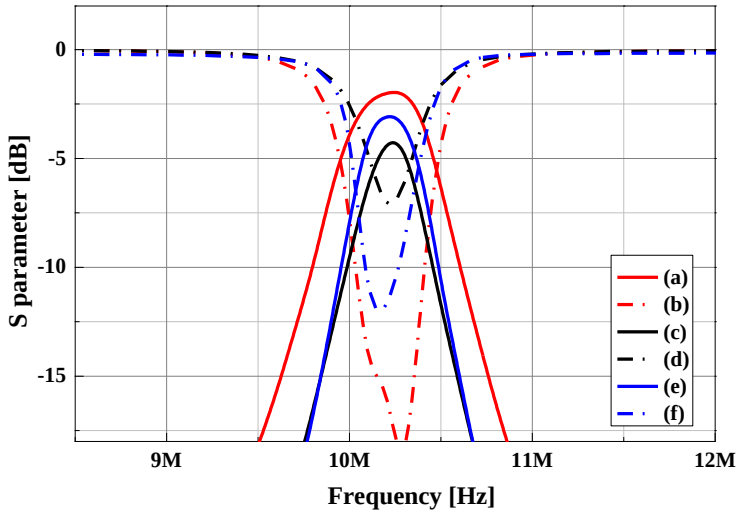


Figure 3-23: Experimental result – measured S parameter.

(a) S21 without axial-misalignment and matching.

(b) S11 without axial-misalignment and matching.

(c) S21 with axial-misalignment and without matching.

(d) S11 with axial-misalignment and without matching.

(f) S21 with axial-misalignment and matching.

# Chapter IV

# Future Works on Antenna-Locked Loop WPT

From the above analysis of the relationship between the system efficiency and the resonant frequency, it is clear that the operating frequency is the critical factor determining the performance of the system. Besides, the flexibility of impedance matching structures also plays an important role enabling high transfer efficiency [25]. Of considerable interest for applications of WPT relied on magnetic resonance, the cases of mobile receiver or multiple receivers are absolutely typical. However, as reported in the previous chapters, there exists a drawback that degenerates the system efficiency in these cases. In fact, the transfer efficiency significantly decreases with distance variations between the transmitter and the receiver or in case of multiple receivers. In order to overcome the limitations, besides the above proposed techniques, the ideas on adaptive circuits are additionally proposed. These circuits are so-called Antenna-Locked Loop (ALL), which help to maintain the optimal resonant condition and realize the maximum wireless power transfer efficiency as well.

## 4.1. Efficiency Optimization based on Frequency Control

For the situation of one transmitter and one portable receiver, the transfer efficiency represented as $|S_{21}|$, which the function of the distance, the relative orientation and alignment between the resonators, is analytically clarified in the chapter II. Remind that magnitude of $S_{21}$ parameter is relatively small when a transmitter and a receiver are too far away. When they get approach each other, $|S_{21}|$ goes up and at a certain point, the phenomenon of frequency splitting occurs degrading the system performance. Therefore, an optimal control mechanism of efficiency based on frequency control is needed to stabilize the transfer efficiency.

Generally, a range of control frequency is confined, with a high limit caused by the coil characteristic and a low limit due to the low efficiency. In that range, the frequency can be determined and tuned in order for high efficiency to be achieved. From the equations (2.7) and (2.8), it is possible to derive a following equation:

$$S_{21} = \frac{j2\omega^3 M_{12} M_{23} M_{34} R_L}{Z_1 Z_2 Z_3 Z_4 + \omega^2 M_{12}^2 Z_3 Z_4 + \omega^2 M_{23}^2 Z_1 Z_4 + \omega^2 M_{34}^2 Z_1 Z_2 + \omega^4 M_{12}^2 M_{34}^2} \tag{4.1}$$

In which mutual inductance $M_{23}$ is calculated by using Neumann formula (Imura & Hori, 2011)

$$M_{23} = \frac{\mu_0}{4\pi} \int_{C_2} \int_{C_3} \frac{dl_2 dl_3}{D} \tag{4.2}$$

However, due to complicated calculations, it is reasonable to use an approximation of the mutual inductance given as below [10]:

$$M_{23} \approx \pi\mu_0 (r_2 r_3)^2 \frac{N_2 N_3}{2D^3} \tag{4.3}$$

Note that in (4.1), typically, almost all components would be identified with given specifications of circuit setup including radius of coils' cross-section a, number of turns N, radius of coils $r_i$ (i=2,3), and distance between the power coil, load coil and resonators. So, by substituting (4.3) into (4.1), there are merely the three unknown variables of frequency ω, $S_{21}$ parameter and distance between the resonators D. With the given requirement of efficiency, represented as the magnitude of $S_{21}$, and identified distance between the resonators, it is able to figure out the frequency of interest. An adaptive circuit used to stabilize the system transfer efficiency is demonstrated in Fig. 4-1. A current sensor is used to detect a current flow in the transmitting coil. Due to the fact that the transmitting coil is not connected to the ground, the sensed signal is in terms of differential signal. The signal is then compared with reference sources in an adjacent block, hence it is essential to utilize a differential amplifier in order to transform the differential signal to a single-ended signal. An output voltage of $V_d$ is then switched to a block of distance identification, where $V_d$ is in turn compared with reference vol-

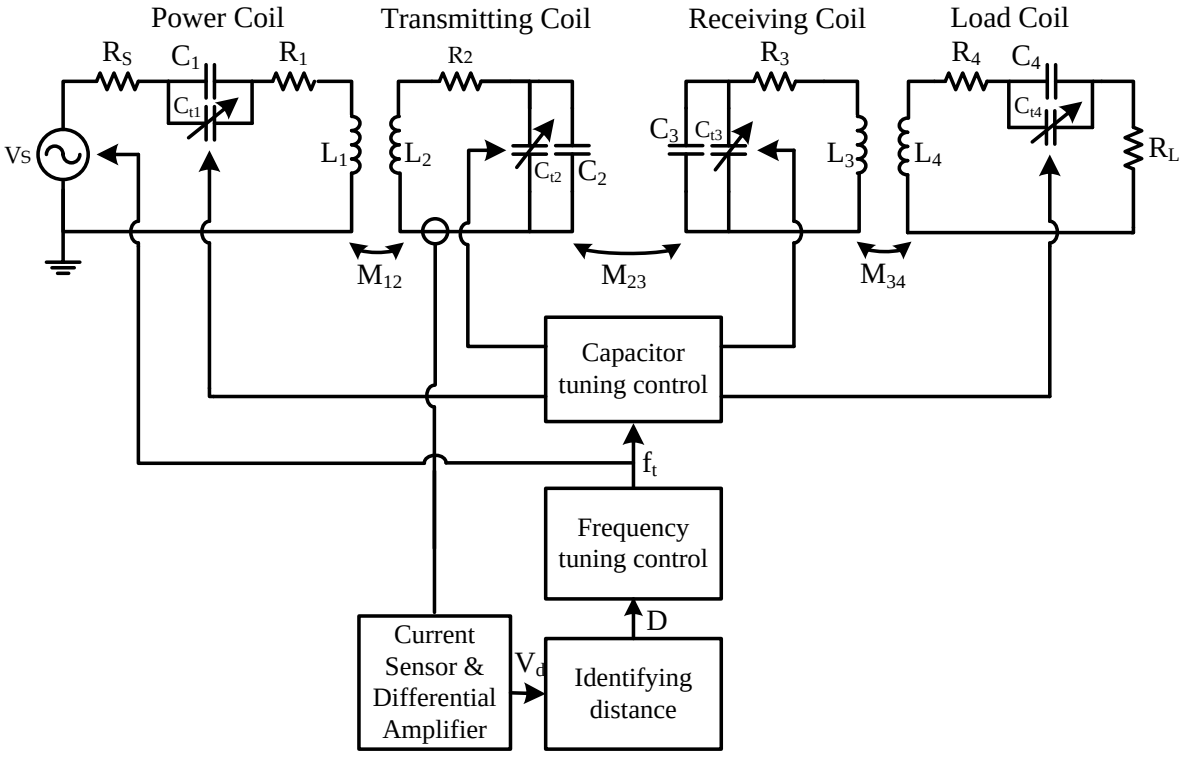


Figure 4-1: Adaptive circuit of frequency control.

tages to determine a distance between the resonators. Like the preceding analysis, with the found parameter, a new tuned $f_t$ is established. This frequency is the wanted frequency of the power source as well. Subsequently, in order to control all coils resonating at the frequency of $f_t$, a capacitor tuning control block is required to control variable capacitors attached at each coil as below

$$f_t = \frac{1}{2\pi L_i C_{total-i}} \ ,i = 1 \sim 4 \tag{4.4}$$

$$C_{ti} = C_{total-i} - C_i \ ,i = 1 \sim 4 \tag{4.5}$$

Note that $C_2$ and $C_3$ here are lumped components representing approximately the parasitic capacitances of the transmitting and receiving coils. The capacitors $C_{ti}$ with i from 1 to 4 are respectively connected in parallel with the capacitors of four coils.

In general, when the frequency tuning mechanism is enabled, the controller picks the resonant frequency of interest and tracks it as the receiver is moved away from the transmitter.

## 4.2. Efficiency Optimization based on Impedance Matching Control

In addition to the efficiency optimization technique based on frequency tuning, impedance matching tuning method is a potential candidate for an adaptive circuit that also maximizes the system efficiency. In some cases, the usage of wide range of frequency tuning has limitations that can affect these other bands such as ISM bands which were internationally reserved. Thus, utilizing the technique of flexible impedance matching is really essential.

In fact, by changing the strength of coupling between the load coil and the resonator and slightly retuning the receiving coil, it is possible to achieve the maximum transfer efficiency (Chen, 2010). For practical interest, however, an adjustment in the coupling coefficient between the coils in the transmitting part is preferred. The change in coupling strength can be made by varying the distance between those coils, the relative orientation and alignment of them. However, it is not viable to automatically control them in the system consisting of four coils. Thus, a model of two resonators and other impedance matching structure is used. A circuit of adaptive impedance matching in the transmitter side is shown in Fig. 4-2. Based on a current sensed from the transmitting resonator, a control circuit block is able to identify distance variations, different orientation, misalignment between the resonators or in case of multiple receivers, then automatically control a power amplifier (PA) and a tunable impedance matching block so as to maximize the transfer efficiency. Actually, for situations of relatively large distance length, significantly different orientation or misalignment between the two resonators, in spite of utilizing the adaptive impedance matching, increasing the out-

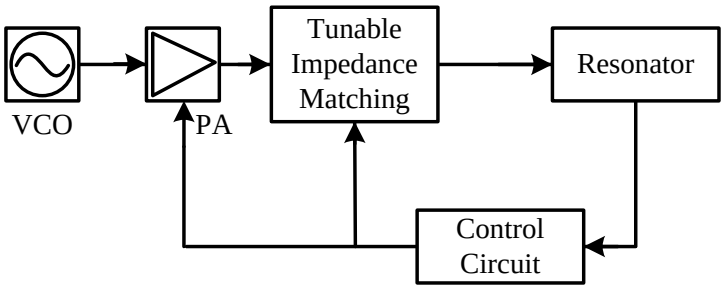


Figure 4-2: Adaptive circuit of impedance matching control in transmitter side.

put power of the power amplifier is recommended to improve the system transfer efficiency. The striking feature of the circuit is that the system frequency is fixed and it is very helpful in many applications.

# Chapter V

# Summary & Conclusion

A general and insightful analysis of WPT systems is presented. Frequency splitting phenomenon is demonstrated by theoretical derivations and simulation results as well. Besides, the comparison between different kinds of coupling and case of multiple receivers are also analyzed to impress the need for adaptive methods to maintain the high performance of the system. Some adaptive methods are proposed and experimental results are described to demonstrate the effectiveness of the proposed methods. The conceptual definition, called Antenna- Locked Loops, offer practical possibilities of WPT with any physical changes. With the wireless power know-how, it is able to counter the transmission of power over distances about tens of feet, although ideally it is very less but still it is impressive. The most interesting fact is that the wireless power transmission is omnidirectional in nature. If the technology is enhanced and sharpened to be a datum where it can be “generative”, it will be able to remain firm to turn the interest of an infinite number of industries. Although, nowadays wireless power is a major obstacle in terms of advancement in the retail sector and also there are many issues regarding the safety, applying and affordability in attentiveness to WPT, but this will likely to be enhanced as the technology further grows up. Generally, this work lays down the ground work of innovative wireless power technology and open opportunities to commercially implement advanced magnetic resonance based WPT systems.

# REFERENCES


1. Tesla, N 1919, 'The True Wireless', *Electrical Experimenter, May*.

2. Tesla, N 1905, 'The Transmission of Electrical Energy Without Wires as a Means for furthering Peace', *Electrical World and Engineer,* Jan.7, p.21.

3. Kurs, A, Karalis, A, Moffatt, R, Joannopoulos, JD, Fiser, P & Soljacic, M 2007, 'Wireless power transfer via strongly coupled magnetic resonances', *Science*, vol.317, pp. 83-86, viewed 1 September 2010,

   http://www.sciencemag.org/content/317/5834/55.full.pdf

4. Basset, P, Kaiser, A, Legrand, B, Collard, D & Buchaillot, L 2007 , 'Complete System for Wireless Powering and Remote Control of Electrostatic Actuators by Inductive Coupling', *Mechatronics, IEEE/ASME Transactions on* , vol.12, no.1, pp.23-31, viewed 30 October 2010,

   http://ieeexplore.ieee.org/stamp/stamp.jsp?tp=&arnumber=4088962&isnumber=4088960

5. Gao, J 2007, "Traveling Magnetic Field for Homogeneous Wireless Power Transmission," *Power Delivery, IEEE Transactions on* , vol.22, no.1, pp.507-514, viewed 30 October 2010,

   http://ieeexplore.ieee.org/stamp/stamp.jsp?tp=&arnumber=4039428&isnumber=4039398

6. Low, ZN, Chinga, RA, Tseng, R & Lin, J 2009, 'Design and Test of a High-Power High-Efficiency Loosely Coupled Planar Wireless Power Transfer System', *Industrial Electronics, IEEE Transactions on* , vol.56, no.5, pp.1801-1812, viewed 10 January 2011,

   http://ieeexplore.ieee.org/stamp/stamp.jsp?tp=&arnumber=4694032&isnumber=4897610

7. Mansor, H, Halim, M, Mashor, M & Rahim, M 2008, 'Application on Wireless Power Transmission for Biomedical Implantable Organ', *Springer-Verlag Biomed 2008 proceedings 21*, pp.40-43, viewed 10 January 2011,

   http://www.springerlink.com/content/h077924v65562846/fulltext.pdf

8. Ishiyama, T, Kanai, Y, Ohwaki, J & Mino, M 2003, 'Impact of a wireless power transmission system using an ultrasonic air transducer for low-power mobile applications', *Ultrasonics, 2003 IEEE Symposium on* , vol.2, no., pp. 1368- 1371, viewed 30 January 2011,

   http://ieeexplore.ieee.org/stamp/stamp.jsp?tp=&arnumber=1293157&isnumber=28794

9. Hongping Hu, Yuantai Hu, Chuanyao Chen & Ji Wang 2008, 'A system of two piezoelectric

transducers and a storage circuit for wireless energy transmission through a thin metal wall', *Ultrasonics, Ferroelectrics and Frequency Control, IEEE Transactions on*, vol.55, no.10, pp.2312-2319, viewed 30 January 2011,

http://ieeexplore.ieee.org/stamp/stamp.jsp?tp=&arnumber=4638917&isnumber=4638892

10. Karalis, A, Joannopoulos, J & Soljacic, M 2008, 'Efficient Wireless Non-radiative Mid-range Energy Transfer', *Elsevier Annals of Physics*, vol.323, no.1, pp34-48, viewed 1 September 2010,

    http://mit.edu/~soljacic/wireless-power_AoP.pdf

11. Blackwell, T 2003, 'Recent demonstrations of Laser power beaming at DFRC and MSFC', *Third International Symposium on Beamed Energy Propulsion, AIP Conference Proceedings*, vol.766, pp.73-85, viewed 30 October 2010,

    http://scitation.aip.org/getpdf/servlet/GetPDFServlet?filetype=pdf&id=APCPCS000766000001000073000001&idtype=cvips&doi=10.1063/1.1925133&prog=normal

12. Theeuwes, JAC, Visser, HJ, van Beurden, MC & Doodeman, GZN 2007, 'Efficient, Compact, Wireless Battery Design', *Wireless Technologies, 2007 European Conference on* , pp.233-236, 8-10, viewed 30 October 2010,

    http://ieeexplore.ieee.org/stamp/stamp.jsp?tp=&arnumber=4403989&isnumber=4403904

13. Benford, J 2008, 'Space Applications of High-Power Microwaves', *Plasma Science, IEEE Transactions on* , vol.36, no.3, pp.569-581, viewed 30 October 2010,

    http://ieeexplore.ieee.org/stamp/stamp.jsp?tp=&arnumber=4539856&isnumber=4539855

14. Shinohara, N & Hashimoto, K 2008, 'Microwave Power Transmission Technologies for SPS, *Journal of the Vacuum Society of Japan*, vol. 51,no. 8, pp. 513-518, viewed 30 October 2010,

    http://www.jstage.jst.go.jp/article/jvsj2/51/8/51_513/_article/-char/ja

15. Matsumoto, H 2002, 'Research on solar power satellites and microwave power transmission in Japan', *Microwave Magazine, IEEE* , vol.3, no.4, pp. 36- 45, viewed 30 October 2010,

    http://ieeexplore.ieee.org/stamp/stamp.jsp?tp=&arnumber=1145674&isnumber=25789

16. http://wirelesspowerconsortium.com

17. Finkenzeller, K 2010, *RFID handbook: fundamentals and applications in contactless smart cards*, 3rd edn, John Wiley and Sons, Inc.

18. Grover, FW 1944, 'The Calculation of the Mutual Inductance of Circular Filaments in Any Desired Positions', *Proceedings of the IRE* , vol.32, no.10, pp. 620- 629, viewed 30 October 2011,

http://ieeexplore.ieee.org/stamp/stamp.jsp?tp=&arnumber=1694856&isnumber=35701

19. Babic, SI, Sirois, F & Akyel, C 2009, 'Validity check of mutual inductance formulas for circular filaments with lateral and angular misalignments', *Progress In Electromagnetics Research M*, vol.8, 15-26, viewed 30 October 2011,

http://www.jpier.org/pierm/pier.php?paper=09060105

20. Akyel, C, Babic, SI & Mahmoudi, MM 2009, 'Mutual inductance calculation for non-coaxial circular air coils with parallel axes', *Progress In Electromagnetics Research*, Vol. 91, pp.287-301, viewed 30 October 2011,

http://www.jpier.org/pier/pier.php?paper=09021907

21. Sengupta, DL & Liepa, VV 2006, *Applied Electromagnetics and Electromagnetic Compatibility*, John Wiley and Sons, Inc.

22. Sample, AP, Meyer, DA & Smith, JR 2011, 'Analysis, Experimental Results, and Range Adaptation of Magnetically Coupled Resonators for Wireless Power Transfer', *Industrial Electronics, IEEE Transactions on* , vol.58, no.2, pp.544-554, viewed 10 May 2011,

http://ieeexplore.ieee.org/stamp/stamp.jsp?tp=&arnumber=5437250&isnumber=5684364

23. Cannon, BL, Hoburg, JF, Stancil, DD & Goldstein, SC 2009, 'Magnetic Resonant Coupling As a Potential Means for Wireless Power Transfer to Multiple Small Receivers', *Power Electronics, IEEE Transactions on* , vol.24, no.7, pp.1819-1825, viewed 10 May 2011,

http://ieeexplore.ieee.org/stamp/stamp.jsp?tp=&arnumber=5175611&isnumber=5075737

24. Lee, J & Shen, C 2007, 'A Comparative Study of Wireless Protocols: Bluetooth, UWB, ZigBee, and Wi-Fi', *33rd Annual Conference of the IEEE, Industrial Electronics Society*, 5-8 November 2007, viewed 10 October 2010,

http://ieeexplore.ieee.org/stamp/stamp.jsp?tp=&arnumber=4460126

25. Chen, CJ, Chu, TH, Lin, CL & Jou, ZC 2010, 'A Study of Loosely Coupled Coils for Wireless Power Transfer', *Circuits and Systems II: Express Briefs, IEEE Transactions on* , vol.57, no.7, pp.536-540, viewed 5 October 2010,

http://ieeexplore.ieee.org/stamp/stamp.jsp?tp=&arnumber=5475182&isnumber=5510051

26. Imura, T & Hori, Y 2011, 'Maximizing Air Gap and Efficiency of Magnetic Resonant Coupling for Wireless Power Transfer Using Equivalent Circuit and Neumann Formula', *Industrial Electronics, IEEE Transactions on* , vol.58, no.10, pp.4746-4752, viewed 1 July 2011,

http://ieeexplore.ieee.org/stamp/stamp.jsp?tp=&arnumber=5709980&isnumber=6005674

27. Ishizaki, T, Fukada, D & Awai, I 2011, 'A novel concept for 2-dimensional free-access wireless power transfer system using asymmetric coupling resonators with different sizes', *Microwave Workshop Series on Innovative Wireless Power Transmission: Technologies, Systems, and Applications (IMWS), 2011 IEEE MTT-S International* , pp.243-246, 12-13, viewed 1 July 2011,

http://ieeexplore.ieee.org/stamp/stamp.jsp?tp=&arnumber=5877121&isnumber=5876647

28. Duong, PT & Lee, JW 2011, 'Experimental Results of High-Efficiency Resonant Coupling Wireless Power Transfer Using a Variable Coupling Method', *Microwave and Wireless Components Letters, IEEE* , vol.21, no.8, pp.442-444, viewed 1 October 2011,

http://ieeexplore.ieee.org/stamp/stamp.jsp?tp=&arnumber=5940188&isnumber=5977170

29. Garnica, J, Casanova, J & Jenshan, L, 'High efficiency midrange wireless power transfer system', *Microwave Workshop Series on Innovative Wireless Power Transmission: Technologies, Systems, and Applications (IMWS), 2011 IEEE MTT-S International* , pp.73-76, 12-13, viewed 1 October 2011,

http://ieeexplore.ieee.org/stamp/stamp.jsp?tp=&arnumber=5877094&isnumber=5876647

30. Pozar, DM 2004, *Microwave Engineering*, 3rd edn, John Wiley & Sons, Inc New York.

# Acknowledgement

First of all, I would like to express my sincere gratitude to my supervisor, Prof. Franklin Bien. His encouragement, inspiration, guidance and support enabled me to develop an understanding of the research. I feel very lucky to be under the direction of Prof. Franklin Bien at UNIST.

Also, I greatly thank Prof. Jingook Kim, Prof. Kijin Han and Prof. Youngmin Kim for their invaluable comments and guidance during the research process. My deep appreciation goes as well to Seunggyu Lee, my co-worker in the WPT project, in addition to Youngsu Kim, Yunho Choi and Sai Kiran Oruganti for their technical assistance and support for the measurements. I would like to thank other BICDL students, who accompanied and encouraged me during my Masters program.

I really appreciate my parents giving me the most valuable affection to study so far.

This work was supported by Basic Science Research Program through the National Research Foundation of Korea (NRF) funded by the Ministry of Education, Science and Technology (grant number 20110005518)